SIAM J. APPL. MATH.
Vol. 50, No. 5, pp. 1373–1418, October 1990
©1990 Society for Industrial and Applied Mathematics
009

ON THE RESONANCE STRUCTURE IN A FORCED EXCITABLE SYSTEM*

JAMES C. ALEXANDER†, EUSEBIUS J. DOEDEL‡, AND HANS G. OTHMER†‡

Abstract. The dynamics of forced excitable systems are studied analytically and numerically with a view toward understanding the resonance or phase-locking structure. In a singular limit the system studied reduces to a discontinuous flow on a two-torus, which in turn gives rise to a set-valued circle map. It is shown how to define rotation numbers for such systems and derive properties analogous to those known for smooth flows. The structure of the phase-locking regions for a Fitzhugh–Nagumo system in the singular limit is also analyzed. A singular perturbation argument shows that some of the general results persist for the nonsingularly-perturbed system, and some numerical results on phase-locking in the forced Fitzhugh–Nagumo equations illustrate this fact. The results explain much of the phase-locking behavior seen experimentally and numerically in forced excitable systems, including the existence of threshold stimuli for phase-locking. The results are compared with known results for forced oscillatory systems.

Key words. Fitzhugh–Nagumo equation, chaotic, excitable system, quasi-periodic, resonance, rotation number, spiking

AMS(MOS) subject classifications. 92A09, 92A40, 34C05, 34C15

1. Introduction.

Many biological and some chemical systems are *excitable*, which means that the equations that describe their temporal evolution in a spatially-uniform system have the following properties: (i) there is a rest point or steady state that is globally attracting relative to some large set in phase space, and (ii), there is a region in state space that can be idealized as a surface of codimension one that locally partitions the phase space into two sets $\mathcal{D}$ and $\mathcal{A}$. The rest point lies in $\mathcal{D}$ (the *decaying set*) and all orbits through initial points in $\mathcal{D}$ return to the rest point without any substantial growth in any of the state variables. Thus an impulsive perturbation of the rest point that leaves the state in $\mathcal{D}$ decays without significant growth, and the responses are called *subthreshold* (cf. Fig. 1). By contrast, perturbations that carry the dynamics into $\mathcal{A}$ (the *amplifying set*) can lead to a large change in one or more of the state variables, even though the system eventually returns to the rest state. Perturbations that carry the state into $\mathcal{A}$ are usually called *superthreshold.* The surface that locally separates the amplifying and decaying sets is called the threshold surface. Examples of models for excitable dynamics include the Fitzhugh–Nagumo equations (Fitzhugh [1969]), the Hodgkin–Huxley equations (Hodgkin and Huxley [1954]), mod-

*Received by the editors December 14, 1987; revision received August 7, 1989; accepted for publication (in revised form) October 30, 1989.

†Department of Mathematics and Institute for Physical Science and Technology, University of Maryland, College Park, Maryland 20742. The work of this author was partially supported by National Science Foundation grant 01523898.

‡Computer Science Department, Concordia University, Montréal, Canada. The work of this author was supported in part by Natural Sciences and Engineering Research Council of Canada grant A4274 and Fonds pour la formation de chercheurs et l'aide a la recherche of Québec grant EQ1438 while he was on leave at California Institute of Technology and Univerity of Utah.

†‡Department of Mathematics, University of Utah, Salt Lake City, Utah 84112. The work of this author was supported in part by National Institute of Health grant GM29123 and grant GR/0/13573 via the Centre for Mathematical Biology, University of Oxford.

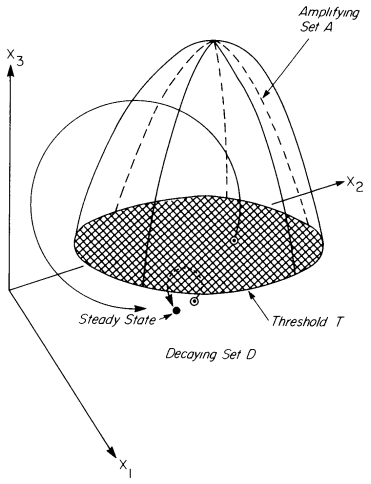

FIG. 1. *A schematic of the phase space for a three-dimensional excitable system. Orbits that begin in the decaying set $\mathcal{D}$ return to the rest point without any significant growth in x_3, whereas along orbits that begin in the amplifying set $\mathcal{A}$ there is a significant amplification in x_3.*

els of the cellular slime mold *Dictyostelium discoideum* (Monk and Othmer [1989]; Othmer and Monk [1988]), the Field–Noyes model of the Zhabotinskii–Belousov reaction (Field and Noyes [1974]), and many others.

It can be anticipated that when an excitable system is forced periodically with a superthreshold stimulus that periodic responses may result, in which case we say that entrainment or phase-locking occurs, in analogy with the similar behavior found in forced oscillatory systems. We shall show that in some cases we can define a firing number or a rotation number which gives the number of superthreshold responses per cycle of the forcing function. When the rotation number is rational and less than one we speak of subharmonic entrainment or subharmonic resonance. Numerous experiments (cf., e.g., Guttman, Feldman, and Jakobsson [1980], Matsumoto et al. [1987], Chialvo and Jalife [1987], and references therein) have been done in which excitable systems were forced periodically, and the results of these experiments show much of the phase-locking structure found in forced oscillatory systems, including apparently chaotic behavior at suitable combinations of the amplitude and frequency of the forcing. An example of the phase-locking regions found in forced excitable cardiac tissue is shown in Fig. 2(a), and some apparently chaotic responses observed under different conditions are shown in Fig. 2(b). Numerical studies on Hodgkin–Huxley systems (Holden [1976]), on a Fitzhugh–Nagumo-like system (Feingold et al. [1988]), and on formal models of neurons (Nagumo and Sato [1972]; Sato [1972]; Sato, Hatta, and Nagumo [1974]), also show that the resonance structure can be quite similar to that in forced periodic systems. The main objective of this paper is to provide a mathematical explanation for the similarities and differences between the phase-locking or resonance structure in forced excitable systems and that in forced oscillatory systems.

In §2 we develop the general model of forced excitable systems that will be analyzed here. The model has slow and fast variables, as is typical of most excitable systems, and in this paper we deal primarily with the singularly-perturbed limit and

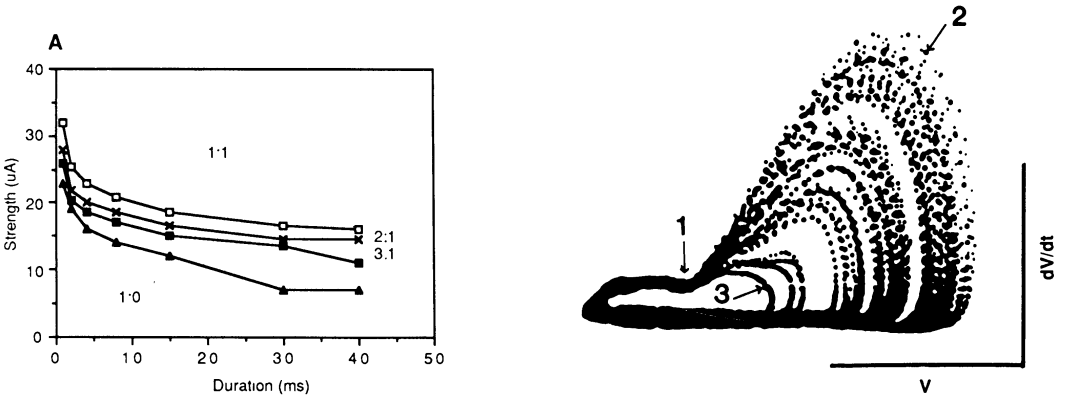

FIG. 2. (a) *Strength-duration curves showing the phase-locking regions in a forced Purkinje fiber. The plot shows the ratio* $p : q$ *of the number of forcing cycles to the number of superthreshold responses for given combinations of the duration of the input pulse in milliseconds and the amplitude in microamps. The period of the forcing is* 700 *milliseconds.* (b) *A map of* 100 *successive pairs of values of the transmembrane potential and its derivative at a forcing frequency of* $322\,\text{min}^{-1}$. *From Chialvo and Jalife* [1987].[1]

small perturbations of this limit. We suppose that the forcing occurs in the equations for the slow variables, but this does not restrict the applicability of the results greatly, for a large class of systems with forcing on the fast variables can be transformed into equations of the form we study. We show in §3 that it is possible to define a rotation number for the singular system and we derive properties of the rotation number. There are some technical hurdles in this analysis because the singular system is not continuous and the orbits are not unique. In fact the associated circle map is set- (or multi-) valued. Thus it is necessary to develop the theory of rotation numbers for multi-valued orbits since this has not been done heretofore to our knowledge. We show that the rotation number depends continuously on parameters and that there are periodic orbits if and only if the rotation number is rational, which is analogous to the classical theory of rotation numbers. Accordingly, for a "random" parameter value, the system will exhibit periodic orbits, which is what is frequently observed in applications. However there are also irrational rotation numbers, which occur as transition states between resonant states, and for these the motion is quasi-periodic. In both the rational and irrational cases, we are able to give an essentially complete description of the asymptotic dynamics.

We next discuss stability of orbits of discontinuous systems on a torus. It is necessary to develop a variational equation for such systems, and although the ideas are straightforward there are some technical details. This development is carried out in §4. In §5 we apply the theories of §§3 and 4 to the singular system of §2 which models

[1]D. R. Chialvo and J. Jalife, *Non-linear dynamics of cardiac excitation and impluse propagation*, Nature, 330 (1987), pp. 749–752. Reprinted by permission of the authors.

a forced excitable system. The dynamics are completely described and it is shown how to investigate stability. We also show in §6 that the phase-locking regions can be easily computed for a piecewise-linear system. In §7 we investigate the nonsingular system. The main result is that for a resonant system the nonsingular dynamics are approximated by the singular dynamics. In particular, the nonsingular system has stable periodic orbits which are uniformly approximated by stable periodic orbits of the singular system.

In §8 we present some numerical results on the forced Fitzhugh–Nagumo equations. The results for this system illustrate both the theory developed in the preceding sections, and what remains to be explained in the transition regions, where chaotic behavior can occur. The latter aspect is currently under investigation. Finally, in §9 we discuss the relationship between our results and previous work. As we shall see there, much of the previous work on discontinuous maps falls within the scope of the theory developed here for discontinous flows.

2. Formulation of the model. The dynamics of excitable systems are typically governed by evolution equations of the form

$$\begin{aligned} \epsilon \frac{dv}{dt} &= f(v, w, \lambda) \\ \frac{dw}{dt} &= g(v, w, \lambda). \end{aligned} \tag{2.1}$$

where $v \in \mathbb{R}^m, w \in \mathbb{R}^n$, $\lambda \in \mathbb{R}^p$ is a parameter vector, and ϵ is small. When $f(v, w, \lambda) \geq O(1)$, v varies rapidly compared with w on the t scale, which implies that the v_i are the fast "voltage-like" variables, and the w_i are the "recovery-like" variables. This form of the equations applies to all the examples mentioned in the Introduction under suitable scalings of the variables.

In the absence of forcing the evolution of the system consists of a rapid motion toward an attracting neighborhood of the set $v = \phi(w, \lambda)$, where $\phi(w, \lambda)$ is such that $f(\phi(w, \lambda), w, \lambda) = 0$, and slower motion in this neighborhood. Locally ϕ defines a smooth $n-$dimensional "slow" manifold when f and g are smooth for fixed λ, but globally $v = \phi(w, \lambda)$ usually has several branches when the system is excitable. As a result, the slow motion in the neighborhood of an attractor may alternate with rapid transitions between different branches. The standard example of such a system is the unforced van der Pol oscillator (Minorsky [1962]).

In general the forcing can enter both the fast and slow subsystems, and it can either enter parametrically, in which case the forcing is state dependent, or additively. Although it is not necessary for our geometric formulation, it is convenient to consider the case for which the forcing enters only through the slow subsystem. This case applies directly to a variety of chemical and biological systems, ranging from the Belousov–Zhabotinskii reaction in a continuous stirred tank reactor (CSTR) with periodic injection of the catalyst to periodically-forced acetylcholine-activated currents in cardiac SA-node tissue (Michaels, Matyas, and Jalife [1984]). (Ostensibly this last reference deals with a forced oscillatory system. However, an analysis shows that the forcing involved is strong enough that the stable attractor is a rest point for part of the forcing cycle. Thus the system studied there falls into the class of excitable systems studied here.) Moreover, the following shows that some general cases of forcing in fast variables can be reduced to this case.

Consider a system of the form

$$\begin{aligned} \epsilon\frac{dv}{dt} &= f\big(v,w,\phi(t)\big) = p(v) - q\big(w,\phi(t)\big), \\ \frac{dw}{dt} &= g(v,w,\psi(t)), \end{aligned} \tag{2.2}$$

with C^1 right-hand sides. In this paper we develop a theory for the case $m = n = 1$; that is, the system (2.2) consists of one fast and one slow equation. Here we assume $m = n = 1$; in the appendix we treat the more general case. Assume that $q_w \neq 0$. Then $\tilde{w} = q(w,\phi)$ is monotone in w for each ϕ and thus there is a function $q = h(\tilde{w},\phi)$ which inverts q for each ϕ. Changing to $(v,\tilde{w})$ variables, the system (2.2) becomes

$$\begin{aligned} \epsilon\frac{dv}{dt} &= p(v) - \tilde{w}, \\ \frac{d\tilde{w}}{dt} &= \frac{\partial q_1}{\partial w} g\big(v, h(\tilde{w},\phi(t)), \psi(t)\big) + \frac{\partial q_1}{\partial \phi}\phi'(t). \end{aligned} \tag{2.3}$$

In these variables, the forcing appears only in the slow variables. Moreover, in each case the transformation is uniform in ϵ and thus is valid in the singular limit $\epsilon \to 0$. As an example note that the Fitzhugh–Nagumo class of equations, which includes the standard cubic nonlinearity in v and piecewise-linear planar excitable systems, are of the type given by (2.2) when the forcing is additive on the fast "voltage-like" variable. As another example, the BZ reaction in a CSTR is often forced by periodic injection of Br^- ion, which is one of the fast variables (Hudson, Lamba, and Mankin [1986]). However, in the FKN model for this reaction such forcing can be transformed to forcing on the slow variable z (which represents Ce^{+4}) by a change of variables of the foregoing type. Finally, the interested reader can check that for Hodgkin–Huxley-like equations, where the voltage and the gating variables enter as products in the voltage equation, the additive forcing $\epsilon\phi(t)$ of the voltage equation can be transformed into forcing of the gating variables by the transformation $v = z + \int \phi(t)$ with a similar transformation for the reversal potentials.

Later we consider the reduction of (2.2) to the singular limit $\epsilon \to 0$, but this reduction is not valid when the forcing frequency is $O(1/\epsilon)$, that is, when the forcing frequency is commensurate with the fast time. In cases like this it also happens that the forcing cannot be isolated on the slow variable, at least not uniformly in ϵ. In fact it is found numerically that new phenomena arise when the frequency of stimulation is comparable to the relaxation rate of the fast variables (Rattay [1986]). Other methods of analysis are required to handle such cases.

The foregoing shows that a number of forced excitable systems can be cast into the form

$$\begin{aligned} \epsilon\frac{dv}{dt} &= f(v,w,\lambda), \\ \frac{dw}{dt} &= g(v,w,\lambda,t) \end{aligned} \tag{2.4}$$

and these are the equations we study in the remainder of this paper. Since the phenomena of interest here arise in planar systems, we only consider the case $m = n = 1$ hereafter. The technical assumptions on (2.4) are as follows.

I. *Smoothness.* The functions $f(v, w, \lambda)$ and $g(v, w, \lambda, t)$ are C^2 in v, w, and λ except possibly at finitely many points, and $g(v, w, \lambda, t)$ is piecewise smooth in t (to allow piecewise constant forcing). For any bounded set U in (v, w)-space and any fixed λ, f, and g are Lipschitz continuous in (u, v), i. e., there is a constant k_U such that

$$\begin{aligned} |f(v, w, \lambda) - f(v', w', \lambda)| &\leq k_U (|v - v'| + |w - w'|) \\ |g(v, w, \lambda, t) - g(v', w', \lambda, t)| &\leq k_U (|v - v'| + |w - w'|) \end{aligned} \tag{2.5}$$

for $(v, w) \in U$. For any initial condition (v_0, w_0, t_0), there is a unique solution of (2.4) for all $t \geq t_0$ (Hale [1969, §I.5]). These solutions depend continuously on (v_0, w_0, λ, t_0).

II. *Conditions on f.* The nullcline $f(v, w, \lambda) = 0$ has the standard "cubic shape" (see Fig. 3). More precisely, we assume that $f(v, w, \lambda) = 0$ can be solved for $w = \gamma(v, \lambda)$ as a continuous function of (v, λ) for every $\lambda \in \Lambda \subset R$, and that

$$\begin{aligned} f(v, w, \lambda) &< 0 \text{ if } w > \gamma(v, \lambda), \\ f(v, w, \lambda) &> 0 \text{ if } w < \gamma(v, \lambda). \end{aligned}$$

Furthermore we assume that there are fixed values $v_l < v_r$ of v such that

$$\begin{aligned} &\gamma(v, \lambda) \text{ is strictly decreasing in } v \text{ for } v < v_l, \\ &\gamma(v, \lambda) \text{ is strictly increasing in } v \text{ for } v_l < v < v_r, \\ &\gamma(v, \lambda) \text{ is strictly decreasing in } v \text{ for } v_r < v, \end{aligned}$$

and that v_l is a nondegenerate minimum for v. That is, there exists $\alpha = \alpha(\lambda) > 0$ such that

$$\gamma(v, \lambda) \geq \gamma(v_l) + \alpha(v - v_l)^2$$

for v near v_l.

Thus $f_w \leq 0$ on the set where $f = 0$, and consequently $f_v \geq 0$ for $v \in (v_l, v_r)$ and $f_v \leq 0$ otherwise.

III. *Conditions on g.* The equation $g(v, w, \lambda, t) = 0$ can be solved for $w = \eta_t(v, \lambda)$ for any fixed t. Moreover, we assume that

$$\begin{aligned} g(v, w, \lambda, t) &< 0 \text{ for } w > \eta_t(v, \lambda), \\ g(v, w, \lambda, t) &> 0 \text{ for } w < \eta_t(v, \lambda). \end{aligned}$$

Thus $g_w \leq 0$ and $g_v \geq 0$ on the set where $g = 0$.

IV. *Transversality.* The nullclines intersect at only one point for any fixed t. That is, for any t and fixed λ there exists a unique solution (v_t^0, w_t^0) to the equations

$$\begin{aligned} w &= \gamma(v, \lambda), \\ w &= \eta_t(v, \lambda). \end{aligned} \tag{2.6}$$

V. *Existence of periodic solutions.* There exist V_l and V_r such that $v_l \leq V_l < V_r \leq v_r$, with the property that whenever the v-component of the rest point of the unforced system lies in (V_l, V_r) the rest point of the unforced system is unstable and the system has a unique periodic solution that is a stable limit cycle. Otherwise the

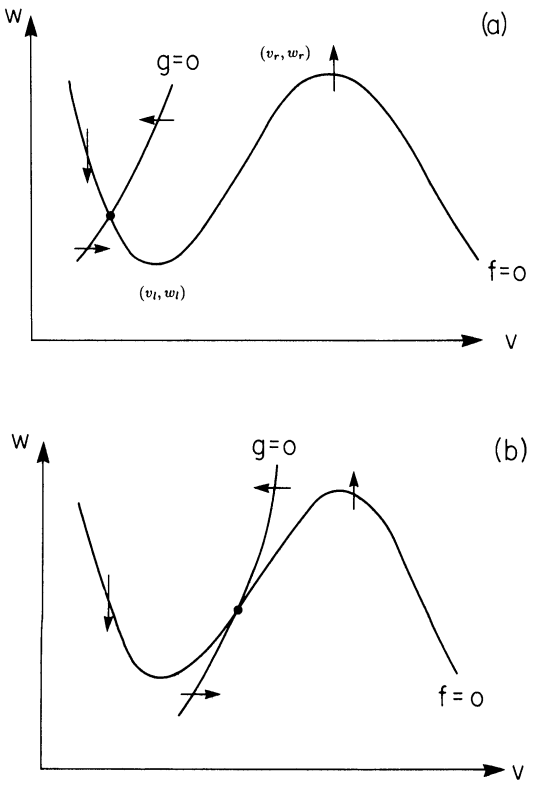

FIG. 3. *The qualitative features of the isoclines $f = 0$ and $g = 0$ when* (a) *the rest point is stable,* (b) *the rest point is unstable. In case* (b) *there is a stable limit cycle which contains the rest point in its interior. The forcing causes the isocline $g = 0$ to move between the two states.*

rest point is asymptotically stable. (Note that V_l and V_r always exist for ϵ sufficiently small, and that $V_l \to v_l$ and $V_r \to v_r$ as $\epsilon \to 0$. Thus this assumption is not necessary for sufficiently stiff systems.)

Next we specify conditions on the forcing. If the forcing is weak in an appropriate sense and the rest point of the unforced system is stable, then under the foregoing conditions it is easy to prove that the forced system will only have small amplitude periodic solutions that are perturbations of the rest point. Such solutions correspond to the subthreshold responses i. e., responses in the region labeled 0: 1 in Fig. 2(a). The only point of mathematical interest in regard to these solutions concerns the nature of the transition region in parameter space between subthreshold and superthreshold responses. An example of such a strength-duration curve is given in §7.

On the other hand, if the amplitude of the forcing is too large there may be an intersection of $g = 0$ with $f = 0$ for $v > v_r$ and we want to exclude this, because it complicates some of the analysis without introducing any significant new phenomena. The last hypothesis ensures that the forcing actually moves the rest point from the left branch of $f = 0$ into the region where it is unstable when regarded as a rest point of the system in which t is fixed in the function g, but does not move it to the right of v_r.

VI. *Conditions on the forcing.* Let $w_l = \gamma(v_l, \lambda)$ and let $w_r = \gamma(v_r, \lambda)$. We assume that $g(v, w, \lambda, t)$ is periodic in t of period $T > 0$, where T is large compared with the time scale for the fast dynamics. Further, we suppose that there exists a $T_1 \in (0, T)$

such that for $t \in (0, T_1)$, $v_t^0 < v_l$, and for $t \in (T_1, T)$, $v_t^0 \in (v_l, v_r)$. Thus there are at most two values of $t \in [0, T)$ at which $(v_t^0, w_t^0) = (v_l, w_l)$. We also assume that in the singular limit $\epsilon = 0$ the forcing turns "on" and "off" rapidly enough. More precisely, if $\gamma'(v_l^+) = 0$, then

$$\lim_{t \to T^-} g_t\big(v_l, \gamma(v_l), \lambda, t\big) > 0 \tag{2.7}$$

(thus the forcing turns off transversally), and if $\gamma'(v_l^-) = 0$, then

$$\big|g_t\big(v_l^-, \gamma(v_l^-), \lambda, T_1^-\big)\big| > \frac{\big[g_v\big(v_l^-, \gamma(v_l^-), \lambda, T_1^-\big)\big]^2}{4\gamma''(v_l^-)} \tag{2.8}$$

(thus the forcing turns on with some nonzero speed). These last two conditions enter certain estimates in a technical way. If they are not satisfied the theory developed here may still be valid, but more technical arguments are necessary.

With these conditions in mind we can describe the qualitative dynamics more completely. Let $\tilde{t}$ and λ be fixed, and consider the autonomous system

$$\begin{aligned} \epsilon \frac{dv}{dt} &= f(v, w, \lambda), \\ \frac{dw}{dt} &= g(v, w, \lambda, \tilde{t}). \end{aligned} \tag{2.9}$$

in which the forcing is frozen. If $v_{\tilde{t}}^0 < v_l$, then $P(\tilde{t}) \equiv (v_{\tilde{t}}^0, w_{\tilde{t}}^0)$ is a globally attracting rest point. If $V_l < v_{\tilde{t}}^0 < V_r$, the rest point $(v_{\tilde{t}}^0, w_{\tilde{t}}^0)$ is unstable, and the unique periodic solution attracts $\mathbb{R}^2 \backslash (v_{\tilde{t}}^0, w_{\tilde{t}}^0)$. Thus if $\tilde{t}$ is regarded as a parameter of the frozen system, a periodic solution emerges or disappears as $\tilde{t}$ changes so that $v_{\tilde{t}}^0$ passes through V_l. For sufficiently small $\epsilon > 0$ the rest point of (2.4) is in the decaying set $\mathcal{D}$ for $0 < t < T_1$, while if $T_1 < t < T$ it is in the amplifying set $\mathcal{A}$. Thus the effect of the forcing is effectively to move the rest point of (2.9) in and out of the amplifying set.

When the forcing varies on the slow time scale, any solution of (2.4) rapidly approaches a stable branch of the set where $f = 0$. For $v_t > V_l$, (2.4) oscillates, and one can count the number of times N that the v-component crosses some value $v^* \geq V_l$ during one period of the forcing. This *firing number* gives the number of large excursions, or *spikes* in one period of the forcing. The firing number may not be the same for each forcing period, and a time average may be taken. Note that the firing number depends on the choice of v^*; there is no canonical choice except in the singular limit. As λ varies, the average firing number may change. As we shall see, it can happen that a new small spike forms and grows as λ changes until it reaches the threshold v^*, in which case the firing number changes discontinuously. Alternatively, there can be a transition region in λ in which there is very complicated periodic, quasi-periodic, or even chaotic behavior. In the singularly-perturbed case $\epsilon = 0$, there is a canonical choice of v^*, and the average firing number is continuous in λ. Moreover, information about the behavior in the transition regions can be developed. The behavior of the singularly-perturbed system will be analyzed in the following sections, followed by some analysis of the non-singularly-perturbed system.

A simple but typical example of a system that exhibits the desired qualitative behavior is one in which the forcing is additive, namely,

$$\begin{aligned} \epsilon \frac{dv}{dt} &= f(v, w), \\ \frac{dw}{dt} &= h(v, w) + \phi(t), \end{aligned} \tag{2.10}$$

for some periodic forcing function $\phi(t)$. It is usually reasonable to consider sinusoîdal forcing, for which $\phi(t) = \sin 2\pi t/T$, or even a step function

$$\phi(t) = \begin{cases} \phi_l & 0 \le t < T_1, \\ \phi_r & T_1 \le t < T, \end{cases} \tag{2.11}$$

where ϕ_l and ϕ_r are such that condition VI above is satisfied. Indeed, there is often little loss in generality in letting $h(v, w)$ be linear, so one can consider the simpler system

$$\epsilon \frac{dv}{dt} = f(v, w),$$
$$\frac{dw}{dt} = v - \alpha w + \phi(t),$$

where α is sufficiently small that condition IV holds.

The first step in the analysis of (2.4) is to set $\epsilon = 0$ and determine the behavior of the resulting singular differential system. We begin this analysis in this section, and to simplify the notation we fix λ for the present and suppress the λ dependence in all formulas.

When $\epsilon = 0$ the equation $\epsilon \dot{v} = f(v, w)$ reduces to the equation $f(v, w) = 0$, or $w = \gamma(v)$. For $v < v_l$ or $v > v_r$, the singular system is on a branch of the nullcline $w = \gamma(v)$. Let $v = \zeta_l(w)$ invert $w = \gamma(v)$ for $v < v_l$ and let $v = \zeta_r(w)$ invert $w = \gamma(v)$ for $v > v_r$. Then the system (2.4) reduces to the discontinuous scalar equation

$$\frac{dw}{dt} = \begin{cases} g(\zeta_l(w), w, t) & \text{for } v = \zeta_l(w) < v_l, \\ g(\zeta_r(w), w, t) & \text{for } v = \zeta_r(w) > v_r. \end{cases} \tag{2.12}$$

If the solution lies on the left branch $v = \zeta_l(w)$ and evolves so that w reaches $w_l = \gamma(v_l)$, it jumps horizontally and instantaneously to the point $(v, w) = (\zeta_r(w_l), w_l)$ on the right branch. Similarly if the solution lies on the right branch $v = \zeta_r(w)$ and w reaches $w_r = \gamma(v_r)$, it jumps horizontally and instantaneously to the point $(v, w) = (\zeta_l(w_r), w_r)$ on the left branch.

Consider the curves

$$L = \{(v, w): v = \zeta_l(w), w_l \le w \le w_r\},$$
$$R = \{(v, w): v = \zeta_r(w), w_l \le w \le w_r\}, \tag{2.13}$$

and identify the endpoints as follows:

$$P_0\colon (v_l, w_l) = (\zeta_l(w_l), w_l) \equiv (\zeta_r(w_l), w_l),$$
$$P_1\colon (v_r, w_r) = (\zeta_r(w_r), w_r) \equiv (\zeta_l(w_r), w_r).$$

The resulting space is a circle S^1, and thus the phase space for (2.12) is the cylinder $S^1 \times R^+$. We let $u \in (0, 1)$ be a coordinate for S^1, where $u = 0 (\equiv 1)$ corresponds to P_0 and some $u_1 \in (0, 1)$ corresponds to P_1. Without loss of generality, we can rescale the time so that the period $T = 1$, and identify the sections $t = 0$ and $t = 1$ of the cylinder. As a result, (2.12) gives rise to the discontinuous equation

$$\frac{du}{dt} = F(u, t) \tag{2.14}$$

on a torus. We transform (2.12) to u coordinates by setting

$$u = \begin{cases} \dfrac{w - w_l}{2W} & \text{for } (v,w) \in R, \\ \dfrac{1}{2} - \dfrac{w - w_r}{2W} & \text{for } (v,w) \in L, \end{cases} \tag{2.15}$$

where $W = w_r - w_l$. Let $u_1 = 1/2$ correspond to w_r. After time is rescaled, (2.12) reads

$$\frac{du}{dt} = \begin{cases} T \cdot F_1(u,t) & \text{for } u \in (0, 1/2), \\ T \cdot F_2(u,t) & \text{for } u \in (1/2, 1). \end{cases} \tag{2.16}$$

Here

$$F_1(u,t) \equiv \frac{1}{2W} g\big(\zeta_r(2Wu + w_l), 2Wu + w_l, Tt\big)$$

$$F_2(u,t) \equiv \frac{-1}{2W} g\big(\zeta_l(-2Wu + W + w_r), -2Wu + W + w_r, Tt\big).$$

Both F_1 and F_2 are extended periodically with period 1 in both t and u. The square $\{(t,u) \in [0,1] \times [0,1]\}$ is a fundamental domain, and the vector field $F(u,t)$ has the following properties on this domain (see Fig. 4).

(i) The horizontal component (i.e., the t-component) is identically 1.

(ii) For $0 < t < t_1, (\equiv T_1/T)$ there is a piecewise-smooth curve given by $u = \overline{P}(t)$ on which the vertical, or u-component, of the vector field vanishes .

(iii) The vertical component is negative for $0 < t < t_1$ and $\overline{P}(t) < u < 1$, it vanishes on $\overline{P}(t)$, and is positive elsewhere. $\overline{P}(t)$ intersects $u = 0$ in at most two points.

(iv) The vector field is continuous except along the lines $u = 0$ $(\equiv 1)$ and $u = 1/2$, and the lines $t = t_c$, where t_c are the t values for which $g(v,w,t)$ of (2.4) is discontinuous. One-sided limits exist and are finite on the lines of discontinuity. For $t \in (0,t_1), F(0^-,t) < 0$, and $F(0^+,t) > 0$, while for $t \in (t_1,1), F(0^-,t) > 0$, and $F(0^+,t) > 0$. For all $t \in (0,1), F(u_1^-,t) > 0$, and $F(u_1^+,t) > 0$.

As we show in the next section, the associated flow is continuous except along the line $u = 0$ $(\equiv 1)$, and standard tools can be adapted to analyze the behavior of the flow.

3. Rotation numbers for multivalued flows. In this section we develop the theory of rotation numbers for flows arising from a class of discontinuous fields. Under certain restrictions on the types of discontinuities admitted, the rotation number turns out to have the same properties as that for smooth flows on tori. The main points of interest for us about the classical theory (Coddington and Levinson [1955, Chap. 17]; Hale [1969, §II.2]; Hartman [1964, §VI.14]) are as follows. Consider the differential equation

$$\frac{du}{dt} = F(u,t) \tag{3.1}$$

in the (t,u)-plane, where F is 1-periodic in both t and u. Equation (3.1) generates a doubly-periodic vector field on the plane with horizontal component identically 1,

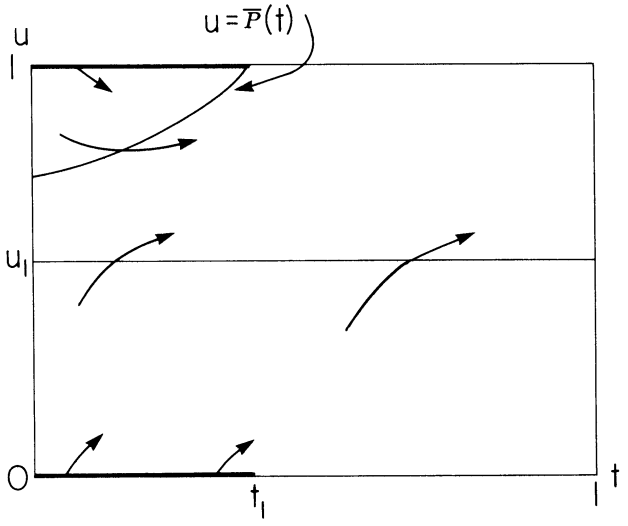

FIG. 4. *The vector field in the fundamental domain of the (t, u) plane. The interval $0 \leq u \leq 1$ consists of two parts—the interval $0 \leq u \leq u_1$, which is a copy of the curve R of (2.12), and the interval $u_1 \leq u \leq 1$, which is an inverted copy of the curve L of (2.12). To recover the vector field on the torus identify the lines $t = 0$ and $t = 1$, and the lines $u = 0$ and $u = 1$. The vertical component of the vector field vanishes along the curve $u = \overline{P}(t)$. This curve is the locus of the moving "stationary" point on the left branch, and in the case shown the amplitude is large enough to force this 'stationary' point across $u = 0$.*

and as in the previous section, we identify this with a vector field on the two-torus T^2 defined as (t, u)-space modulo the unit lattice. Let $C^0(T^2)$ denote the set of continuous, doubly-periodic vector fields on T^2 with the property that solutions of (3.1) through any point on T^2 are unique, and endow this set with the C^0 topology. The time-one map of (3.1) generates a monotone increasing homeomorphism Ψ on R with the property that $\Psi(x+1) = \Psi(x) + 1$. The rotation number of any point $x \in R$ is defined as

$$\rho(x) = \lim_{|n| \to \infty} \frac{\Psi^n(x)}{n},$$

which has the properties:

(i) ρ is well-defined and is independent of x,

(ii) there is a closed orbit on the torus if and only if ρ is rational,

(iii) ρ depends continuously on $F \in C^0(T^2)$.

In the present case, the vector fields are only piecewise continuous and orbits are not unique, and thus the classical theory does not apply directly. Furthermore, the induced circle map is set-valued and therefore more recent results on the properties of rotation numbers for continuous nondecreasing maps on S^1 (Newhouse, Palis, and Takens [1983]) are also not applicable. We suppose that the vector fields are piecewise smooth in the sense that $F(u, t)$ is C^k for $k \geq 1$ except along certain lines. We assume that $F(u, t)$ extends continuously along these lines and that the one-sided limits of the derivatives exist in the generalized sense that some of the limits may be infinite. These exceptional lines are classified as follows.

(i) *Space discontinuities.* There are a finite number (up to periodicity) of values $u = u_c$ such that

$$\Delta F(u_c, t) = \Delta_{u_c} F(u_c, t) = F(u_c^+, t) - F(u_c^-, t) \neq 0. \tag{3.2}$$

We assume that $F(u_c^+, t)$ and $F(u_c^-, t)$ are piecewise smooth in t (jumping only at points t_c).

(ii) *Time discontinuities.* There are a finite number (up to periodicity) of values $t = t_c$ such that

$$\Delta F(u, t_c) = \Delta_{t_c} F(u, t_c) = F(u, t_c^+) - F(u, t_c^-) \neq 0. \tag{3.3}$$

We assume that $F(u, t_c^+)$ and $F(u, t_c^-)$ are piecewise smooth in u (jumping only at points u_c).

Thus (t, u)-space is partitioned into a collection of rectangles by the horizontal lines $u = u_c$ and the vertical lines $t = t_c$. We call these lines the *lines of discontinuity* of $F(u, t)$. $F(u, t)$ is smooth in the open rectangles and for any such rectangle R, $F(u, t)$ can be extended to a continuous function on the closure of R. Therefore the standard existence and uniqueness theorems (Coddington and Levinson [1955, Chaps. 1 and 2]; Hale [1969, §I.3]; Hartman [1964, Chap. 2]) imply that (3.1) has a unique solution through any point (t_0, u_0) not on a line $u = u_c$, and this solution depends continuously on the initial conditions. We denote this solution $U(t, t_0, u_0)$. For multivalued solutions $U(t, t_0, u_0)$ is interpreted as a set. We use the notation $U(t, t_0, u_0, \lambda)$ if we want to explicitly denote the parameter.

Since F is bounded a solution $U(t, t_0, u_0)$ for u_0 not on a line $u = u_c$ can be extended in both directions to a line $u = u_c$ (although it will have corners at lines $t = t_c$). We require that the partial derivatives F_u and F_t extend continuously to one-sided derivatives at any line of discontinuity, and we allow F_u to become positively or negatively infinite along these lines. It is easy to show, using Gronwall's inequality, that for any point (t, u) in ∂R where F_u is not infinite at most one orbit through (t, u) intersects the interior of R. In fact, more is true. Even if F_u is infinite at $(t, u) \in \partial R$, at most one orbit through (t, u) intersects the interior of R unless $F(u, t) = 0$ as well. For if not, apply Gronwall's inequality to $dt/du = 1/F(u, t)$.

The nature of the flow near the lines $u = u_c$ is determined by the sign of $F(u, t)$ above and below such a line. We first consider the cases in which the signs of F are constant on an open interval around t_* and then we patch such regions together at points where F changes sign and at time discontinuities. Fix $t_* \in (t_1, t_2)$, where (t_1, t_2) is chosen so that there is no time discontinuity in this interval, and let $F^{\pm}(u_c, t_*)$ denote the limits from above and below (t_*, u_c). Choose (t_1, t_2) so that $\operatorname{sgn}\big(F^+(u_c, t)\big)$ is constant (including 0) for $t \in (t_1, t_2)$, and similarly for $\operatorname{sgn}\big(F^-(u_c, t)\big)$. If the sign is 0, assume $F_u(u_c, t) \neq 0$ for $t \in (t_1, t_2)$. Then there are nine distinct cases to be considered, depending on whether $F^{\pm}$ is $+, -$, or 0. We shall only sketch the analysis of these cases and leave the details to the reader. A summary of the cases is given in Table 1 and sketches of some of the associated orbits are shown in Fig. 5. In the systems discussed in §2 there are no instances of sign 0, and $F(u_c, t)$ and $F_u(u_c, t)$ vanish simultaneously only at isolated points.

If $F(u_c^+, t_*) \cdot F(u_c^-, t_*) > 0$ the orbit has a unique extension forward and backward in time across $u = u_c$, although with a corner at $t = t_*$ (Fig. 5(a)). We call these

TABLE 1
The orbit structure when $\operatorname{sgn}(F^{\pm})$ *is fixed.*

$\operatorname{sgn}(F^-)$	$\operatorname{sgn}(F^+)$	Type	Uniqueness*	
			Forward	Backward
+	+	Transverse	Yes	Yes
−	−	Transverse	Yes	Yes
+	−	Attracting	Yes	No
−	−	Repelling	No	Yes
0	0		Yes	Yes
0	+		Yes	Yes
0	−		Yes	Yes
+	0		Yes	Yes
−	0		Yes	Yes

* Refers to uniqueness through any point (t, u_c), $t \in (t_1, t_2)$.

transverse space discontinuities because the trajectories intersect the line of discontinuity transversely. If $F(u_c^+, t_*) < 0$ and $F(u_c^-, t_*) > 0$, $u = u_c$ is locally attracting in the sense that solutions are decreasing for $u > u_c$ and increasing for $u < u_c$. In this case two orbits can reach $u = u_c$ at $t = t_*$, one from above and one from below, and for $t > t_*$ these orbits continue *along* the line $u = u_c$ (Fig. 5(b)). The solution through (t_*, u_c) is locally (in t) unique for $t > t_c$, but is not unique in reverse time. On the other hand, if $F(u_c^+, t_*) > 0$ and $F(u_c^-, t_*) < 0$, the line $u = u_c$ is locally repelling near t_*, and a solution that begins in the interior of either adjacent rectangle cannot reach (t_*, u_c) in forward time. However, it can be shown that solutions which begin near (t_*, u_c) can reach (t_*, u_c) from either above or below in finite reverse time. Thus there are two solutions that emanate immediately from (t_*, u_c) into the interior of rectangles R, one that lies above the line $u = u_c$ and one that lies below the line $u = u_c$. In addition, we also consider any orbit that travels along $u = u_c$ for some interval of time to (t_*', u_c) and then (with a corner) goes into the interior of a rectangle R to be an orbit from (t_*, u_c). In this case the solution through (t_*, u_c) is unique locally for $t < t_c$, but is not unique in forward time. Note that the dynamics near attracting and repelling space discontinuities are related by reversing time.

In the remaining "constant sign" cases one or both of the limits vanish for $t \in (t_1, t_2)$. Suppose, for example, that F^- vanishes. Since the horizontal component of the vector field is 1, orbits cannot reach (t_*, u_c) from below, and there is always a unique orbit through (t_*, u_c). Using this observation we can complete the table for these cases. Finally, at the intersection of a space discontinuity $u = u_c$ and a time discontinuity $t = t_c$, we simply patch together the orbit types given in Table 1 at $t = t_c$.

In all cases for which the orbit through a point on $u = u_c$ is not unique, we regard the forward extension of the orbit to be the set of *all* orbits that emanate from this point. This includes orbits which may "travel along" the discontinuity $u = u_c$ for some finite interval of time. More precisely, for any point (t_0, u_0), let $\mathcal{S}^+(t_0, u_0)$ denote the set of all forward orbits with (t_0, u_0) as initial point, and let $\overline{u}(t) = \sup\{u \in \mathcal{S}^+(t_0, u_0)\}$ and $\underline{u}(t) = \inf\{u \in \mathcal{S}^+(t_0, u_0)\}$. Since the supremum and

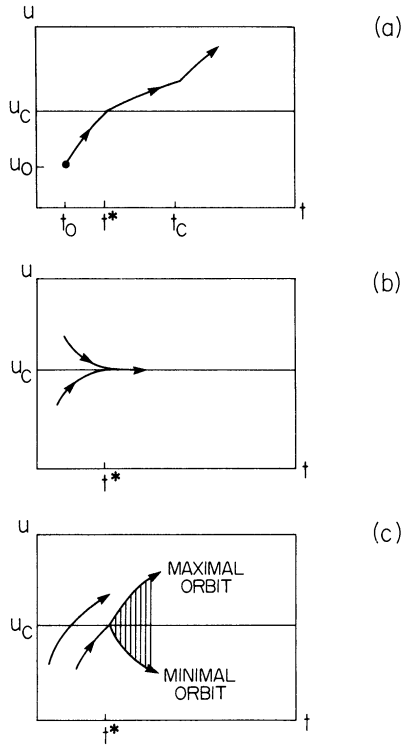

FIG. 5. *A schematic of the behavior of solutions near the various types of discontinuities.* (a) *The flow near a transverse space discontinuity at* $u = u_c$. *The orbit through* $(u,t) = (u_0, t_0)$ *reaches the discontinuity at* $t = t^*$. *The line* $t = t_c$ *is a time discontinuity.* (b) *The flow near an attracting space discontinuity at* $u = u_c$. *An orbit that reaches the line* $u = u_c$ *at* $t = t^*$ *continues along that line for* $t > t^*$. (c) *A space discontinuity that is transverse for* $t < t^*$ *and repelling for* $t > t^*$. *There is a maximal orbit and a minimal orbit leaving* $(u,t) = (u_c, t^*)$, *and the hatched region between these orbits is called the forward shadow of the point* (u_c, t^*).

infimum of orbits are orbits, $\overline{u}(t)$ and $\underline{u}(t)$ are orbits in $\mathcal{S}^+(t_0, u_0)$, called the *maximal* and *minimal* orbits, respectively (Hartman [1964, §III.2]). We call the set of points in the plane between the minimal and maximal forward orbits through a point the *forward shadow* of that point. Since the horizontal component of the vector field is identically 1, the forward shadow of the point (t_0, u_0) is $\mathcal{S}^+(t_0, u_0)$. *Backward shadows* and *full (or two-sided) shadows* are defined similarly. We also speak of $\mathcal{S}^+(t_0, u_0)$ *at time* t_1 $(\geq t_0)$ and by this mean the section of the shadow at t_1. If there is only one orbit through a point, the forward shadow consists of all points on the positive semiorbit through that point.

In this way the discontinuous vector field under consideration defines a set-valued flow in the plane and, by factoring modulo the integer lattice, a set-valued flow on the torus T^2. However, a rotation number cannot be defined for these flows unless the following condition holds: for any (t_0, u_0),

$$\mathcal{S}^+(t_0, u_0) \cap \mathcal{S}^+(t_0, u_0 + 1) = \emptyset. \tag{3.4}$$

The fact that this condition is necessary can be seen as follows. Because the orbit through an interior point of a rectangle is unique, this condition can only be violated if the shadows intersect on a space discontinuity. If (3.4) is not satisfied and the two

shadows intersect at time t_1, then *all* orbits are contained in $\mathcal{S}^+(t_0, u)$ for $t \geq t_1$ and all $u \in [u_0, u_0 + 1]$. As a result, $\mathcal{S}^+(t_0, u)$ contains the whole torus for $t \geq t_1$ and *any* u, and there can be no theory of rotation numbers. Thus we are led to impose the following additional hypothesis on (3.1):

(H1) *There are no attracting space discontinuities and there is at most one orbit emanating in reverse time from any point at which F_u is infinite.*

As discussed above, the second part of (H1) is an issue only at space discontinuities and only if F is zero at the point in question. It follows from the preceding discussion that under this hypothesis uniqueness holds for the time-reversed flow, but not in general for the forward flow. The backward uniqueness implies that (3.1) is satisfied and, as we show next, rotation numbers can be defined satisfactorily in this case.

Let $\Psi(u_0) \equiv U(1, 0, u_0)$ denote the time one map for (3.1). This map has the property that

$$\Psi(u_0 + n) = \Psi(u_0) + n$$

for $n \in Z$, where the equality is defined setwise when u lies on a line $u = u_c$. That is, if $(\Psi^-(u_c), \Psi^+(u_c))$ is the image of u_c, then the foregoing means that

$$\big(\Psi^-(u_c + n), \Psi^+(u_c + n)\big) = \big(\Psi^-(u_c) + n, \Psi^+(u_c) + n\big).$$

Furthermore, Ψ is monotone in the usual sense. We define the *rotation number* ρ as

$$\rho = \lim_{|n| \to \infty} \frac{\Psi^n(u_0)}{n}, \tag{3.5}$$

where $n \in \mathbf{Z}$. We claim that the value of ρ is independent of u_0 and of the choice of the orbit through $(0, u_0)$. To see this, let $\overline{U}(t, 0, u_0)$ be the maximal orbit through $(0, u_0)$ and let $U^1(t, 0, u_0) = U(t, 0, u_0) + 1$. By periodicity in u, $U^1(t, u_0)$ is also a solution of (3.1). Moreover

$$U(n, 0, u_0) \leq \overline{U}(n, 0, u_0) < U^1(n, 0, u_0) = U(n, 0, u_0) + 1, \tag{3.6}$$

where the second inequality comes from (3.4). Dividing by n and taking the limit, we find that ρ does not depend on which orbit is chosen through $(0, u_0)$. With this fact, the argument in Coddington and Levinson [1955] and in Hale [1969] can be used mutatis mutandi, replacing $U(t, u_0 + m)$ by the m-translate $U^m(t, 0, u_0) = U(t, 0, u_0) + m$ for $-\infty < m < \infty$. Thus the rotation number ρ is well-defined.

The rotation number also has properties (ii) and (iii) given previously. We prove (iii) only for one-parameter families of vector fields, and we define continuity with respect to a parameter λ to mean that the lines $u_c = u_c(\lambda)$ and $t_c = t_c(\lambda)$ depend continuously on λ, and away from any such line the vector field depends continuously on λ.

THEOREM 1. *Under condition* (H1):

(i) *ρ is rational if and only if there is a closed orbit of the differential equation* (3.1) *on the torus,*

(ii) *if the vector field depends continuously on λ then so does ρ.*

Proof. Certainly if there is a closed orbit of (3.1), then for some integer $m > 0$ and some u_0 there is an integer k such that $U(m, 0, u_0) = u_0 + k$, which implies that

$\rho = k/m$. To prove the converse, note that if $U(m, 0, u_0) > u_0 + r$ for all u_0 for some real number r, then $\rho > r/m$. For by induction on l,

$$U(lm, 0, u_0) > U\big((l-1)m, 0, u_0\big) + r > u_0 + lr.$$

Dividing by lm and letting $l \to \infty$, we obtain the inequality. Now suppose $\rho = k/m$ for integers k and m, but that $U(m, 0, u_0) \neq u_0 + k$ for any u_0. We may suppose that $U(m, 0, u_0) > u_0 + k$. But then $\rho > k/m$ by what was just proved, contrary to assumption. Thus $U(m, 0, u_0) = u_0 + k$ and there is a closed orbit on the torus.

For (ii), we use the following trick. Rotation numbers can also be defined for the time-reversed flow (indeed, since reverse orbits are unique as a consequence of (H), the standard arguments work). Moreover, the rotation numbers for the forward flow and the time-reversed flow are equal (note that n changes to $-n$ in (3.5)). Thus we prove continuity of the reverse rotation number. Continuous dependence of rotation numbers on a parameter depends on the continuous dependence of orbits on the parameter. Suppose (3.1) depends continuously on a parameter λ. Denote the unique orbit for parameter value λ through the point u_0 and time t_0 for $t \leq t_0$ by $U(t_0, t, u_0, \lambda)$. By periodicity, the orbit is uniformly continuous in the following sense: for fixed $T_1 < T_2$, given $\epsilon > 0$, there exists a $\delta = \delta(T_1, T_2, \lambda) > 0$ such that

$$|U(t_0, t, u_0, \lambda) - U(t_0', t', u_0', \lambda')| < \epsilon \tag{3.7}$$

if $T_1 \leq t \leq t_0 \leq T_2$, $T_1 \leq t' \leq t_0' \leq T_2$, and $|t_0 - t_0'| < \delta$, $|t - t'| < \delta$, $|u_0 - u_0'| < \delta$, $|\lambda - \lambda'| < \delta$. This is true within any rectangle R where F is continuous (Hartman [1964, §V.2]). Then (3.6) can be applied iteratively over rectangles. Now let $t_0' = t_0$, $t' = t = t_0 - 1$, $u_0' = u_0$. Then given $\epsilon > 0$, there exists $\delta > 0$ such that if $|\lambda' - \lambda| < \delta$, then

$$|U(t_0, t_0 - 1, u_0, \lambda) - U(t_0, t_0 - 1, u_0, \lambda')| < \epsilon.$$

By induction on k

$$|U(t_0, t_0 - k, u_0, \lambda) - U(t_0, t_0 - k, u_0, \lambda')| < k\epsilon.$$

Dividing by k and taking limits, we obtain that $|\rho(\lambda) - \rho(\lambda')| \leq \epsilon$ if $|\lambda' - \lambda| < \delta$, which implies that ρ is continuous in λ. This completes the sketch of the proof.

Finally we observe that *if ρ is rational, then as $t \to \infty$ any orbit whose shadow does not eventually (for times $t \geq$ some t_1) contain a periodic orbit must approach a periodic orbit as $t \to \infty$* (and similarly for $t \to -\infty$). For since ρ is rational, there exists an orbit $U(t, 0, u_0)$ such that $U(n, 0, u_0) = u_0 + k$ for integers n and k. Consider the shifted return maps $\underline{g}: u_0 \mapsto \underline{U}(n, 0, u_0) - k$ and $\overline{g}: u_0 \mapsto \overline{U}(n, 0, u_0) - k$. These are monotonic in u_0. Consider any u_0, $0 \leq u_0 \leq 1$. If $\underline{g}(u_0) \leq u_0$ and $\overline{g}(u_0) \geq u_0$, the forward shadow of u_0 contains a periodic orbit. Otherwise assume $1 \geq \underline{g}(u_0) > u_0$. If the forward shadow of u_0 does not eventually contain a periodic orbit, then, by induction on r, $1 \geq \overline{g}^r(u_0) \geq \underline{g}^r(u_0) > \underline{g}^{r+1}(u_0)$, and both $\underline{g}^r(u_0)$ and $\overline{g}^r(u_0)$ must approach the same point u_1, $0 < u_1 \leq 1$, and $\underline{U}(t, 0, u_1)$ is a periodic orbit. Note that the approach to the periodic orbit is locally monotonic.

4. Variational equations for discontinuous vector fields. In this section we study the stability of solutions of (4.1). As usual we make use of the variational equation, but because the underlying vector field is discontinuous some care is needed in the analysis of this equation.

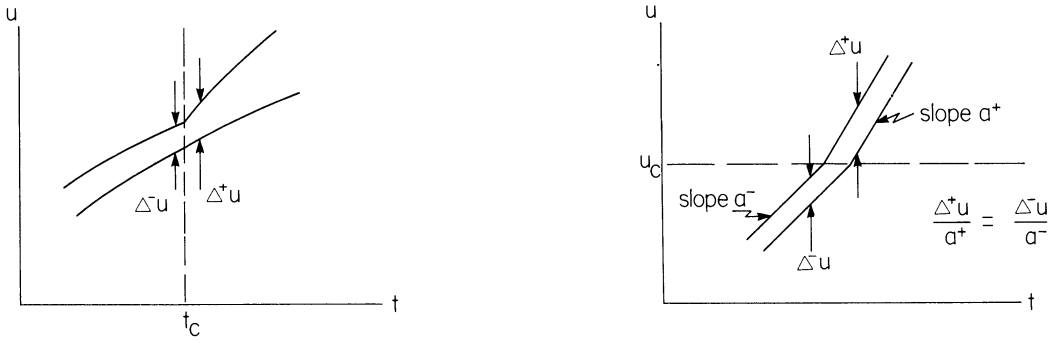

FIG. 6. (a) *Infinitesimally close orbits crossing a time discontinuity* $t = t_c$. *There is no effect of* t_c *on the variation in that* $\lim \Delta^- u = \lim \Delta^+ u$. (b) *Infinitesimally close orbits crossing a space discontinuity. The effect on the variation is given by* (4.4).

We begin with the equation (3.1):

$$\frac{du}{dt} = F(u,t). \tag{4.1}$$

As before, we assume that $F(u,t)$ is piecewise smooth in the sense that there are a finite number of discontinuities of the types defined in the previous section that occur along lines in (t,u)-space. In the open rectangles defined by these lines, $F(u,t)$ is smooth and for each such rectangle R, $F(u,t)$ can be extended to a smooth function on the closure of R, except that F_u may become infinite. An orbit may intersect the corner of a rectangle and hence encounter a space discontinuity and time discontinuity simultaneously, but it will be shown that the effects of the two discontinuities can be considered separately. We restrict our attention to orbits $u(t)$ for which $F\big(u(t),t\big) \neq 0$ for all t; such orbits are single-valued.

If $u(t)$ is a solution of (4.1), the variational equation should describe the behavior of an infinitesimally nearby solution. More precisely we have to determine how a solution $u(t) + \epsilon\xi(t)$ behaves as ϵ goes to zero. Since $F(u,t)$ is C^k for $k \geq 1$ in the interior of any R,

$$\frac{d\big(u(t)+\epsilon\xi(t)\big)}{dt} = F\big(u(t)+\epsilon\xi(t),t\big) = F\big(u(t),t\big) + \epsilon\frac{\partial F}{\partial u}\big(u(t),t\big)\xi + O(\epsilon^2) \tag{4.2}$$

for $u \neq u_c$, $t \neq t_c$, and the variational equation reads

$$\frac{d\xi}{dt} = \frac{\partial F}{\partial u}(u,t)\xi \tag{4.3}$$

for (t,u) in any R.

First we analyze the effect of having a time discontinuity at $t = t_c$. Let $\Delta^- u = \epsilon\xi(t_c^-)$ and $\Delta^+ u = \epsilon\xi(t_c^+)$ be the difference between u and a nearby solution $u + \Delta u$ on the left and right of $t = t_c$, respectively. Since the line of discontinuity is vertical, $\Delta^+ u = \Delta^- u$ (see Fig. 6(a)), which implies that the time discontinuity has no effect on the dynamics of ξ.

Next suppose that there is a space discontinuity at $u = u_c$, and suppose that an orbit $U(t)$ reaches this discontinuity at $t = t_{u_c}$. Since $F(u_c^+, t_{u_c})$ and $F(u_c^-, t_{u_c})$ are not zero, we can invert the relationship $u = U(t)$ to obtain $t = \tau(u)$, where $d\tau/du = F(u,t)^{-1}$ (in other words, the roles of space and time as dependent and independent variables are interchanged locally). From the previous paragraph, $\Delta^+\tau = \Delta^-\tau$. On the other hand, the difference quotient $\Delta u/\Delta\tau$ approaches $du/dt = F\big(u, \tau(u)\big)$ as $\Delta\tau$ goes to zero. Thus (compare Fig. 6(b))

$$\frac{\Delta^+ u}{F(u_c^+, t_{u_c})} = \frac{\Delta^- u}{F(u_c^-, t_{u_c})}. \tag{4.4}$$

Now consider a solution $u = u(t)$ of (4.1) between the times $t = t_0$ and $t = t_1$. For convenience, we assume $u(t_i)$, $i = 1, 2$ does not lie on a line of discontinuity. Integrating (4.3) and taking into account (4.4), we find that

$$\frac{\xi(t_1)}{\xi(t_0)} = \prod_c \frac{F(u_c^+, t_{u_c})}{F(u_c^-, t_{u_c})} \exp\left(\int_{t_0}^{t_1} \frac{\partial F}{\partial u}(u,t)\, dt\right), \tag{4.5}$$

where the product is over all space discontinuities encountered by $u(t)$ and the integral ignores the discontinuities. We can rewrite (4.5) as follows if we leave the integration of (4.3) in logarithmic form. Let $\Delta \log|\xi| = \Delta_{t_0}^{t_1} \log|\xi| = \log|\xi(t_1)| - \log|\xi(t_0)|$ and $\Delta \log|F(u_c, t_{u_c})| = \log\big|F(u_c^+, t_{u_c})\big| - \log\big|F(u_c^-, t_{u_c})\big|$. Then

$$\Delta \log|\xi| = \sum_c \Delta \log|F(u_c, t_{u_c})| + \int_{t_0}^{t_1} \frac{\partial F}{\partial u}(u,t)\, dt. \tag{4.6}$$

It will be convenient to have (4.6) in another form. First suppose that $F\big(u(t), t\big) \neq 0$ for $t_0 \leq t \leq t_1$. Note that along u,

$$\frac{dF}{dt}\big(u(t), t\big) = \frac{\partial F}{\partial u}(u,t)\dot{u} + \frac{\partial F}{\partial t}(u,t). \tag{4.7}$$

Thus we can divide (4.3) by ξ and by $\dot{u}(t) = F(u(t), t)$ and integrate between t_0 and t_1 to obtain

$$\Delta \log|\xi| = \Delta \log|F| - \int_{t_0}^{t_1} \frac{\partial \log|F|}{\partial t}(u,t)\, dt, \tag{4.8}$$

where $\Delta \log|F| = \Delta_{t_0}^{t_1} \log|F| = \log|F(u(t_1), t_1)| - \log|F(u(t_0), t_0)|$. We have to interpret the integral on the right at lines of discontinuity so that (4.8) is consistent with (4.6). To do this, we isolate a small interval around each line of discontinuity and compare the two equations. We find that space discontinuities do not affect the integral on the right of (4.8), but that each time discontinuity t_c adds a term $\Delta \log\big|F\big(u(t_c), t_c\big)\big| = \log\big|F\big(u(t_c^+), t_c^+\big)\big| - \log\big|F\big(u(t_c^-), t_c^-\big)\big|$ to the right-hand side. Thus the integral in (4.8) is a generalized integral in the sense of distributions, and each time discontinuity introduces a Dirac delta function in the logarithmic derivative. Written as an ordinary integral with the same conventions (4.6), (4.8) reads

$$\Delta \log|\xi| = \Delta \log|F| - \sum_c \Delta \log\big|F\big(u(t_c), t_c\big)\big| - \int_{t_0}^{t_1} \frac{\partial \log|F|}{\partial t}(u,t)\, dt. \tag{4.9}$$

Finally there is the question of what happens if $F\big(u(t),t\big)=0$ at a point on the orbit u. It can be checked that if $dF\big(u(t),t\big)/dt \neq 0$ at such a point, the integral in (4.8) should be interpreted as a principal value and the singularity causes no trouble. If $F\big(u(t),t\big)=0$ on an open t-interval (so that the orbit remains on a stationary point for some interval of time), it is better to use (4.5).

The following special cases illustrate some of the foregoing alternatives. Suppose that (4.1) is autonomous, so that $\partial F/\partial t \equiv 0$. Then from (4.8)

$$\Delta \log|\xi| = \Delta \log|F|\,, \tag{4.10}$$

in accordance with the usual results. On the other hand, if (4.1) is independent of u, then from (4.4),

$$\Delta \log|\xi| = 0 \tag{4.11}$$

(the system is invariant under vertical translations). Suppose that $F\big(u(t_1),t_1\big) = F\big(u(t_0),t_0\big)$ (as is the case for a periodic orbit). Then from (4.9)

$$\Delta \log|\xi| = -\sum_c \Delta \log\big|F\big(u(t_c),t_c\big)\big| - \int_{t_0}^{t_1} \frac{\partial \log|F|}{\partial t}(u,t)\,dt. \tag{4.12}$$

For a periodic orbit of an autonomous system,

$$\Delta \log|\xi| = 0 \tag{4.13}$$

as can be seen by considering an autonomous system on a circle.

Finally we note that if $u(t)$ is a periodic orbit of (4.1) and $\Delta \log|\xi| \neq 0$, then the orbit is hyperbolic and thus persists under perturbations of the system.

5. The resonance structure in the singular limit. In this section we apply the general results from the previous two sections to the system (2.12), which is the singularly-perturbed limit of (2.1). As we proved in §3, (3.1) has a periodic solution if and only if the rotation number is rational. When $\rho = n/m$ with m and n coprime, we say that the system is phase-locked in the ratio $n\colon m$ or that it is in an $n\colon m$ resonance, and we use $\mathcal{R}_{n/m}$ to denote the $n\colon m$ resonance zone in parameter space. The same definitions can be used in the forced oscillatory case, and in that case a great deal is known about the structure of the resonance zones. Consider the autonomous system in R^k

$$\frac{du}{dt} = f(u)$$

and suppose that this has an asymptotically stable periodic solution of period 1. The forced system

$$\frac{du}{dt} = f(u) + Ag(u,\omega t),$$

where $g(u,t)$ is periodic of period 1 in t, has a periodic solution for every rational value of ω when $A=0$. Furthermore, the resonance zones, or Arnold tongues, are generically wedge-shaped regions that emanate from $(n/m,0)$ in the (ω,A) plane (Hall [1984]; Loud [1967]). Some recent results on how these tongues interact at large amplitude forcing are given in Mackay and Tresser [1986]. As stated in the introduction, one of our purposes is to determine the structure of the resonance zones of forced excitable

systems. In this section we do this for the singular limit in a three-parameter family of additively-forced systems. Some analytical and numerical results on the nonsingular limit are given in the following two sections.

The first step is to show that the theory developed in §3 applies to the class of equations discussed in §2. In particular, we establish the following lemma.

LEMMA 2. *Equation* (2.16) *satisfies hypothesis* (H1) *of* §3.

Proof. According to property (IV) in §2, the vector field is continuous except along the lines $u = 0$ and $u = 1/2$, and along the lines $t = t_c$ that arise from discontinuities in the forcing. F_u may become infinite along the lines $u = 0$ and $u = 1/2$, but $F(1/2, t)$ is never 0, and $F(0, t)$ can only be 0 if $t = 0$ or $t = t_1$. The segment $(0, t_1)$ on $u = 0$ is repelling and the segment $(t_1, 1)$ is transverse (see Table 1). The line $u = 1/2$ is a transverse discontinuity for all t and plays no significant role in determining the dynamics. Furthermore, it is easy to see from the discussion in §3 that time discontinuities across which the flow does not change type also have little effect. Thus we only have to check the behavior of the flow near $(0, 0)$ and $(t_1, 0)$ in order to determine whether backward orbits are unique. In fact it suffices to check the one-sided behavior for $u = 0^-$.

From (2.15), the variables u and w are linearly related on each rectangle. Accordingly, we can work with the system (2.12), which can be written

$$\frac{dw}{dt} = K(t, w) = g(\zeta_l(w), w, t) \tag{5.1}$$

for $v \leq v_l$, which is the region of interest (recall that the λ dependence is supressed in the notation). Note that

$$\frac{\partial K}{\partial w} = \frac{\partial g}{\partial v}\frac{\partial \zeta_l}{\partial w} + \frac{\partial g}{\partial w} = \left(\frac{\partial f}{\partial v}\right)^{-1} \det \begin{pmatrix} \frac{\partial f}{\partial v} & \frac{\partial f}{\partial w} \\ \frac{\partial g}{\partial v} & \frac{\partial g}{\partial w} \end{pmatrix},$$

since

$$\frac{\partial \zeta_l}{\partial w} = -\frac{\partial f}{\partial w} \Big/ \frac{\partial f}{\partial v}.$$

Thus the right-hand side of (5.1) may have infinite derivative at $v = v_l$ if $f_v \to 0$ as $v \to v_l$ from the left. If not (e.g., if there is a corner of $\gamma(v)$ at v_l, or if $\partial f/\partial v$ and $\partial f/\partial w$ both go to zero at the same rate), uniqueness in reverse time obtains. However, if $\gamma'(v) \to 0$ as $v \to v_l$ from the left, we change variables from w to $v = \zeta_l(v)$ and obtain the equation

$$\frac{dv}{dt} = J(t, v) = \frac{g\big(v, \gamma(v), t\big)}{\gamma'(v)}. \tag{5.2}$$

Introduce a new independent variable τ and write (5.2) as the autonomous system

$$\begin{aligned} \frac{dt}{d\tau} &= -\gamma'(v), \\ \frac{dv}{d\tau} &= -g(v, \gamma(v), t). \end{aligned} \tag{5.3}$$

Then $dt/d\tau \geq 0$ and is 0 only at $v = v_l$. Moreover, (5.3) is C^1 and so has unique (forward and reverse) orbits. However, if the point (T, v_l) or (T_1, v_l) is a stationary

point of (5.3) there may be many orbits which are asymptotic to it in forward τ time. In t time, this occurs in finite time, and (5.2) and hence (5.1) do not have unique orbits in reverse time. To check this possibility we linearize (5.3) and obtain the matrix

$$\begin{pmatrix} 0 & -\frac{d^2\gamma}{dv^2} \\ -\frac{\partial g}{\partial t} & -\frac{\partial g}{\partial v} - \frac{\partial g}{\partial w}\frac{\partial \gamma}{\partial v} \end{pmatrix}. \tag{5.4}$$

At $(T,0)$ this has sign structure

$$\begin{pmatrix} 0 & - \\ - & \leq 0 \end{pmatrix}$$

by virtue of (§2.II, eq. (2.7)). Thus the determinant of (5.4) is negative and $(T,0)$ is a saddle of (5.3). Thus there is only one orbit of (5.3) positively asymptotic to the fixed point from the quadrant $t < T$, $v \leq v_l$. On the other hand, at $(T_1,0)$, the matrix (5.4) has the sign structure

$$\begin{pmatrix} 0 & - \\ + & \leq 0 \end{pmatrix}$$

and $(T_1,0)$ is a center or attracting node or spiral. It is a center or spiral if (2.8) holds. In this case, there are no orbits asymptotic to the fixed point from the quadrant $t < T_1$, $v < v_l$. Thus reverse orbits are unique and the lemma is proved.

Remark. If the opposite inequality in (2.8) holds, there are certainly orbits asymptotic to the fixed point from the quadrant $t < T_1$, $v < v_l$, and reverse orbits are not unique. However, depending on the behavior of g, these orbits may collapse in reverse time to a single orbit at $(0,0)$. In this case, the theory of this paper is still valid. If not, the theory must be extended.

We call the forward shadow of the point (0,0) the *critical shadow*, and any orbit through $(0,0)$ will be called a *critical orbit.* If the interior of the critical shadow contains a lattice point (m,n) (Fig. 7(a)), one of the orbits in the critical shadow is periodic and the rotation number is n/m. Let $u^+ \equiv \overline{U}(1,0,0)$ (respectively, $u^- \equiv \underline{U}(1,0,0)$), and let u_0 be such that $U(m-1,0,u_0) = 0$; then there is a periodic solution of rotation number n/m if $u_0 \in (u^-,u^+)$. For some of the analysis it is more convenient to use the circle map $\mathcal{T}$ induced by the time-one map Ψ. $\mathcal{T}$ is set-valued at 0 because $\mathcal{T}\colon 0 \to I^1 \equiv (\alpha_1,\beta_1) \subset S^1$, and is an orientation-preserving homeomorphism on $(0,1)$ because orbits through points in $(0,1)$ are unique (Fig. 7(b)). $\mathcal{T}^{-1}$ is point-valued but has a flat spot whenever the critical shadow at $t = 1$ is an interval.

Let $\mathcal{T}_0 \equiv \{\mathcal{T}^p(0) : p \in Z^-\}$ be the set of preimages of 0. This is a countable set since backward orbits are unique. It is clear that whenever the critical shadow is an interval the set $(0,1) \setminus \mathcal{T}_0$ is contracted by the factor $1 - |(\alpha_1,\beta_1)|$ per iterate, where $|I|$ denotes the length of the interval I. However, this is not sharp enough for our purposes, and in order to give a more complete description of the dynamics we introduce another hypothesis. Suppose that the following *contraction hypothesis* for the time-one map Ψ, and hence for the circle map $\mathcal{T}$, holds: *there is a* $p \geq 1$ *such that* Ψ^p *is a uniform contraction on any interval* J *where it is point-valued,* in the sense that there is a $\delta > 0$ such that each $J_0 \subset J$ of length l is mapped to a subinterval of length $\leq (1-\delta)l$. When Ψ satisfies this hypothesis we call it a p-contraction. The time-one map of Fig. 7(b) is not a 1-contraction since it has slope larger than 1 near $u = 1$. However the second iterate is a contraction where it is point-valued.

To understand the meaning of this hypothesis, recall that along any orbit we have

$$\frac{\xi(t_1)}{\xi(t_0)} = \prod_c \frac{F(u_c^+,t_{u_c})}{F(u_c^-,t_{u_c})} \exp\left(\int_{t_0}^{t_1} \frac{\partial F}{\partial u}(u,t)\,dt\right). \tag{5.5}$$

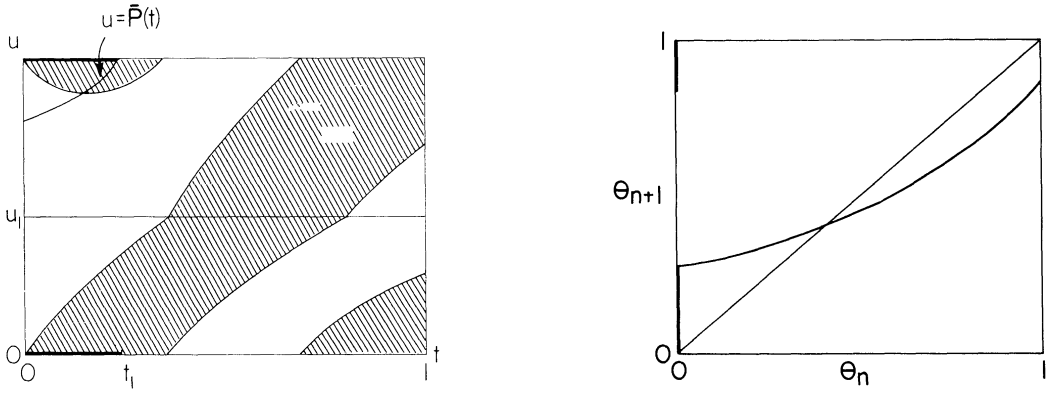

FIG. 7. (a) *The forward shadow of the origin at time* 1, *translated into the fundamental domain* $[0,1] \times [0,1]$. *The critical shadow contains the lattice point* $(1,1)$. (b) *The graph of the circle map* $\mathcal{T}$ *induced by the time one map of the flow.*

It is easy to show, using the hypotheses on g given in §2, that $F_u < 0$ in the interior of any rectangle R, and therefore the exponential factor is always less than 1. Thus an interval around a fixed orbit contracts under the flow if the cumulative product of the jumps encountered, which is always positive, is less than the contraction that occurs in the interior of the rectangles traversed. The hypothesis states that this need not be true for $t_1 = 1$, but only that there is an integer p such that it holds for $t_1 = p$.

THEOREM 2. *Suppose that* Ψ *is an* m*-contraction.*

I. *If the lattice point* (m,n), m *and* n *coprime, lies in the interior of the critical shadow then:*

(i) *there is a unique periodic solution (up to translation in* t *by* k *for* $k = 1, \cdots, m-1$*) of* (2.12) *in the critical shadow and it is unstable (this conclusion does not require that* Ψ *be an* m*-contraction),*

(ii) *there is a unique periodic solution (up to translation in* t *by* k *for* $k = 1, \cdots, m-1$*) of* (2.12) *outside the critical shadow and it is asymptotically stable.*

II. *If the critical shadow does not contain a periodic orbit then* (2.12) *has no periodic solution.*

Proof. It suffices to suppose that $(m,n) = (1,1)$ for the proof of (i) and (ii); the proof for other (m,n) is very similar. The uniqueness of the orbit in the critical shadow is a consequence of the uniqueness of backward orbits. That it is unstable follows from the nonuniqueness of the forward orbit through (0,0). The existence and uniqueness of the stable orbit follows from the fact that Ψ (or $\mathcal{T}$) is an m-contraction on intervals on which it is point-valued. If the critical shadow does not contain a periodic orbit then it does not contain a lattice point, and $0 \notin \mathcal{T}^k(0)$ for any k. Since $\mathcal{T}^m$ is a 1-contraction, and since $\mathcal{T}^m(0,1)$ covers $[0,1] \backslash \mathcal{T}^m(0)$, it follows that there are no fixed points of $\mathcal{T}^m \in (0,1)$.

Remark. The trivial nonuniqueness of the stable periodic solutions only obtains

for the flow on R^2; there is a unique stable closed orbit on T^2.

Next consider the case in which the rotation number is irrational. Let $I^p = \text{int}\{\mathcal{T}(I^{p-1})\} \equiv (\alpha_p, \beta_p)$ for $p \in Z^+$. In this case $I^p \cap \{0\} = \phi$, for otherwise there is a periodic orbit of period $p+1$. Furthermore, the intervals I^p are disjoint, for if $I^p \cap I^q \neq \phi$ there is a periodic orbit of period $p-q$. When $p > 0$ the arcs I^p are arranged monotonically on S^1 because $\mathcal{T}$ is monotone where it is point-valued (cf. Fig. 8).

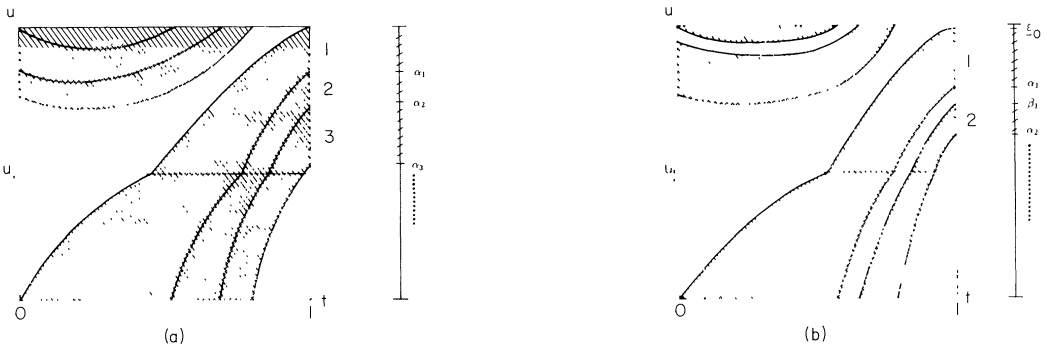

FIG. 8. *The shadow in the fundamental domain and on the section* $t \equiv 0 \pmod 1$. *In case* (a), *the maximal orbit emanating from the point* $(0,0)$ *hits the point* $(1,1) \equiv (0,0)$. *The successive iterates of the shadow on the section* $t \equiv 0 \pmod 1$ *fill up the section from the "top" down without gaps between. In case* (b) *the maximal orbit crosses just below the point* $(1,1)$. *In this case, there are small gaps between successive images of the shadow on the section. Later images lie in these gaps. If the shadow does not contain any lattice point* (n,m) *with* $n > 0$, *the images fill in all of the section except for a Cantor set and the rotation number is an irrational number slightly less than* 1. *Alternatively some lattice point* (n,m) *for large* n *is contained in the shadow and the rotation number is the rational* m/n *near* 1.

Clearly there is no limit point in any of these arcs, for otherwise there would be a periodic solution. It follows that the α- and ω-limit set of any point in $(0,1) \setminus \mathcal{T}_0$ lies in the set

$$\mathcal{C} \equiv \left(\mathcal{T}_0 \cup_{p=0}^{\infty} I^p\right)^c.$$

The set $\mathcal{C}$ is nonempty and invariant by construction, and when the contraction hypothesis holds $\mathcal{C}$ contains no interval, since $|\mathcal{T}^n\{(0,1) \setminus \mathcal{T}_0\}| \to 0$ as $n \to \infty$. If $s \in \mathcal{C}$ is an α_n for some $n \in Z^+$, then it follows from the monotonicity of the arcs I^p that there is an increasing subsequence $\{\alpha_{n_k}\}$ converging to α_n. A similar argument applies for any β_n, and together this shows that every endpoint is a limit point of $\mathcal{C}$. If $s \in \mathcal{C}$ is not an endpoint then $s = \lim_{n_k \to \infty} \alpha_{n_k}$ for some subsequence $\{\alpha_{n_k}\}$, since $\mathcal{C}$ has empty interior. Therefore $\mathcal{C}$ is perfect and has empty interior, i.e., it is a Cantor set.

When the contraction hypothesis holds and ρ is irrational the dynamics on the Cantor set can be described completely. Suppose that each of the intervals I^p is identified to a point. The quotient space is also a circle (note that $0 \equiv 1$ is not in any of the intervals). For any Cantor set on the interval $[0,1]$ consider a continuous monotonic Cantor function f which is constant on each component of the complement

of the Cantor set and strictly monotonic on the Cantor set. The space obtained by collapsing each component of the complement is homeomorphic to $f([0,1])$. The time 1 map induces a dynamical system on the quotient space with the same rotation number (this follows from a definition of rotation number which depends only on the local ordering of the circle, and not on any notion of angle (Guckenheimer and Holmes [1983, §6.2])). Denjoy's theory (Denjoy [1932]) (see Theorem 17.3.2 of Coddington and Levinson [1955] or Theorem II.2.3 of Hale [1969]) implies that on this circle the dynamics are conjugate to rotation by the angle $2\pi\rho$. This proves the first part of the following theorem.

THEOREM 3. *Suppose that the contraction hypothesis holds and that the rotation number is irrational. Then every noncritical orbit is dense in the complement of the critical shadow. The rotation number is stable under perturbations in* (2.12) *if and only if the critical shadow contains a lattice point in its interior. If* (2.12) *depends continuously on parameters, then on the boundaries in parameter space of a phase-locking region for rotation number n/m either the maximal orbit or the minimal orbit of the critical shadow at $t = m$ passes through the lattice point (m,n).*

The proof of the statements concerning the behavior of the rotation number under perturbations is left to the reader.

In general it is difficult to prove that the contraction condition holds, since it is usually impossible to intergrate the variational equations analytically. Thus it is usually necessary to check the contraction condition numerically, but for sufficiently simple systems it may be possible to make the necessary estimates. We outline one possibility.

Consider the singular limit of (2.10) with a step function forcing. This can be written in terms of the coordinate u as follows.

$$\dot{u} = f(u) + \phi(t) \equiv F(u,t), \tag{5.6}$$

where $\phi(t)$ is as in (2.11). Suppose a periodic orbit has rotation number $n/1$, which means that there are n spikes during a forcing cycle. Note that for $T_1 < t < T$, (5.2) is effectively autonomous, since $\phi(t) \equiv \phi_r$ is constant there. It follows from (5.5) that the orbit is asymptotically stable if

$$\left|\frac{f\big(u(T_1^-)\big) + \phi_l}{f\big(u(T^+)\big) + \phi_l}\right| \cdot \left|\frac{f\big(u(T^-)\big) + \phi_r}{f\big(u(T_1^+)\big) + \phi_r}\right| < 1. \tag{5.7}$$

The second term in the product is bounded since $f\big(u(T_1^+)\big) + \phi_r$ can be bounded away from 0, and the first term can be controlled by controlling $T_1 - T$. In particular, when $t \in (0, T_1)$ the rest point on L is asymptotically stable by the properties of §2, and thus the numerator of the first factor can be made sufficiently small by making T_1 sufficiently large. In other words, if the decaying phase $\mathcal{D}$ is sufficiently long (depending on f), (5.7) holds.

If the forcing is not a step function such explicit bounds will not be available. In particular, $F(u, T_1^+)$ can be zero. However, if $T_1 - T$ is sufficiently large and the change in the forcing from the decaying set to the amplifying set is sufficiently fast (in particular if $F'(u, T_1)$ is large enough), it will be possible to control $F(u(T_1), T_1)$ and similar results can be obtained.

6. The structure of the resonance zones. According to Theorem 2, when the contraction hypothesis holds, (2.14) has a periodic solution if and only if the critical

shadow contains a periodic orbit, which, by Theorem 1, is true if and only if the rotation number is rational. Thus the parameter set for which the critical shadow contains a lattice point (m, n) coincides with $\mathcal{R}_{n/m}$. According to Theorem 1, if the vector field depends continuously on a parameter then the rotation number does also, and therefore it is constant on open intervals of the parameter. In this case Theorem 2 states that when the parameter lies on the boundary of $\mathcal{R}_{n/m}$ either the maximal or the minimal orbit of the critical shadow passes through the lattice point (m, n), and a saddle-node bifurcation of periodic solutions occurs at this parameter value. Consequently, the boundaries of the resonance zones can be determined analytically (up to solving certain transcendental equations) for additive step forcing. In this section, we carry out the determination of the resonance zones for this case.

Suppose that the contraction hypothesis is satisfied and suppose that (2.12) has the form

$$\frac{dw}{dt} = \begin{cases} g(\zeta_l(w), w) - f(t) & \text{for } v = \zeta_l(w) < v_l, \\ g(\zeta_r(w), w) - f(t) & \text{for } v = \zeta_r(w) > v_r. \end{cases} \tag{6.1}$$

where f is piecewise constant and takes the values 0 and $\overline{A}$. Clearly there is threshold value $\overline{A}_0$ of $\overline{A}$, below which the solution never reaches the right branch even if the forcing is always on, and this value is

$$\overline{A}_0 = g(\zeta_l(w_l), w_l).$$

The minimum time t_0 needed to reach threshold from any point $w_0 \in (w_l, w_r)$ for any $\overline{A} > \overline{A}_0$ is given by

$$T_t = \int_{w_0}^{w_l} \frac{dw}{g(\zeta_l(w), w) - \overline{A}} \equiv \Theta(\overline{A}).$$

It is clear that $\Theta'(\overline{A}) < 0$, and thus the resulting strength-duration relationship $\overline{A} = \Theta^{-1}(T_t)$ is qualitatively similar to the boundary of the 0:1 region given in Fig. 2 for periodic forcing.

Now suppose that the forcing is given by the periodic extension of period T of the function

$$\overline{f}(t) = \begin{cases} 0 & \text{for } t \in (0, T_1), \\ \overline{A} & \text{for } t \in (T_1, T). \end{cases}$$

Condition VI in §2 is satisfied only if $\overline{A} < \overline{A}_1 \equiv g(\zeta_r(w_r), w_r)$. If $T_1 = 0$ then (6.1) has a periodic solution of period $T_0(\overline{A})$ (or frequency $\omega(\overline{A})$) when regarded as an autonomous equation, but it is only periodic as a solution of the nonautonomous equation with trivial time-dependence if $T/T_0(\overline{A})$ is rational.

It is convenient to transform the equations to u coordinates as is §2. Let θ denote the fraction of the unit interval during which the forcing is off. Then (2.16) becomes

$$\frac{du}{dt} = \begin{cases} T(F_1(u) - f(t, \theta)) & \text{for } u \in (0, 1/2), \\ T(F_2(u) + f(t, \theta)) & \text{for } u \in (1/2, 1), \end{cases} \tag{6.2}$$

and

$$f(t, \theta) = \begin{cases} 0 & \text{for } t \in (0, \theta), \\ A & \text{for } t \in (\theta, 1). \end{cases}$$

The threshold value of A is denoted A_0 and the upper bound on A, above which the rest point lies on the right branch of $f = 0$, is denoted A_1.

Equation (6.2) has a solution of period m at $\theta = 0$ if $T/T_0 = n/m$, or equivalently, if $\omega_0/\omega = n/m$, where $\omega = 2\pi/T$. When this resonance condition is satisfied at $\theta = 0$ the flow on T^2 is parallel and the critical shadow reduces to a single orbit. If $\theta > 0$ and $A > A_0$, $\mathcal{S}^+(0,0)$ intersects $t = 1$ in an interval, and the boundaries of $\mathcal{R}_{n/m}$ in the (ω, θ) plane correspond to the (ω, θ) pairs for which either the maximal orbit or the minimal orbit passes through (m, n). We sketch the analysis needed to determine these boundaries for $(m, n) = (1, 1)$ and leave the general case to the reader.

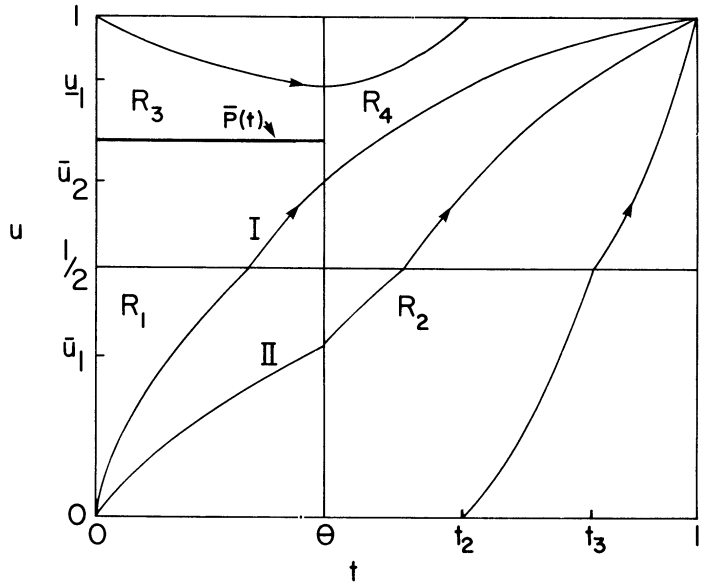

FIG. 9. *A sketch of the paths for the maximal and minimal orbits (see Fig. 8) through* $(1,1)$ *when* (ω, θ) *lies on the corresponding boundary of the* 1:1 *resonance zone.*

Consider the minimal orbit through $(0,0)$. This leaves the rectangle R_3 (cf. Fig. 9) at a point $(0, \underline{u}_1)$ and enters R_4. In order for this orbit to pass through $(1,1)$, it must either remain in R_4 and pass through $(1,1)$, or it must leave R_4, enter R_2, and then enter R_4 again. The former case is included as a limiting case of the latter. Let $(\theta, \underline{u}_1), (t_2, 1)$ and $(t_3, 1/2)$ denote the exit point from R_3, R_4 and R_2, respectively. These points depend on (ω, θ, A) but the sequence $R_3 \to R_4 \to R_2 \to R_4$ is the same whenever the minimal orbit passes through $(1,1)$. This sequence defines the sequence of maps $\mathcal{F}_i$ such that

$$(0,0) \xrightarrow{\mathcal{F}_1^-} (\theta, \underline{u}_1) \xrightarrow{\mathcal{F}_2^-} (t_2, 1) \xrightarrow{\mathcal{F}_3^-} (t_3, \frac{1}{2}) \xrightarrow{\mathcal{F}_4^-} (1,1).$$

The composition of these maps yields an equation $\mathcal{F}^- = 0$ that defines one boundary of $\mathcal{R}_{1/1}$. We find that $\mathcal{F}^-$ is given by

$$\mathcal{F}^-(\omega, \theta, A) = 1 - \frac{\omega}{2\pi}\left[\int_1^{\underline{u}_1(\omega,\theta)} \frac{du}{F_2(u)} + \int_{\underline{u}_1(\omega,\theta)}^1 \frac{du}{F_2(u) + A} + \int_0^{\frac{1}{2}} \frac{du}{F_1(u) - A} + \int_{\frac{1}{2}}^1 \frac{du}{F_2(u) + A}\right], \tag{6.3}$$

where $\underline{u}_1(\omega,\theta)$ is defined by

$$\theta = \frac{\omega}{2\pi}\int_1^{\underline{u}_1(\omega,\theta)} \frac{du}{F_2(u)}.$$

Note that $\underline{u}_1(\omega,\theta)$ is independent of A and depends on (ω,θ) only through $z \equiv \theta/\omega$.

Now suppose that $A \in (A_0, A_1)$ is fixed. It follows from the second equation that

$$\frac{\partial \underline{u}_1}{\partial \omega}(\omega,\theta) > 0$$

and that

$$\frac{\partial \underline{u}_1}{\partial \theta}(\omega,\theta) < 0.$$

From these it follows that

$$\frac{d\theta}{d\omega} = -\frac{\mathcal{F}^-_\omega}{\mathcal{F}^-_\theta} < 0$$

along the curve defined by $\mathcal{F}^- = 0$.

A similar procedure can be followed for the maximal orbit through $(0,0)$ to determine $\mathcal{F}^+$. Now however, there are two distinct sequences through the rectangles $R_1,\cdots,R_4$, and this implies that the part of the boundary of $\mathcal{R}_{1/1}$ determined by the condition that the maximal orbit passes through $(1,1)$ is only piecewise C^1. (Indeed it is true in general that the boundaries of $\mathcal{R}_{n/m}$ are piecewise smooth, and that discontinuities in the derivatives may arise when the the transition sequence $R_i \to R_j \to \cdots \to R_k$ changes at discrete values of (ω,θ).)

We find that

$$\mathcal{F}^+_I(\omega,\theta,A) = 1 - \frac{\omega}{2\pi}\left[\int_0^{1/2}\frac{du}{F_1(u)} + \int_{1/2}^{\overline{u}_2(\omega,\theta)}\frac{du}{F_2(u)} + \int_{\overline{u}_2(\omega,\theta)}^{1}\frac{du}{F_2(u)+A}\right] \tag{6.4}$$

for $z > z^*$, and

$$\mathcal{F}^+_{II}(\omega,\theta,A) = 1 - \frac{\omega}{2\pi}\left[\int_0^{\overline{u}_1(\omega,\theta)}\frac{du}{F_1(u)} + \int_{\overline{u}_1(\omega,\theta)}^{\frac{1}{2}}\frac{du}{F_1(u)-A} + \int_{\frac{1}{2}}^{1}\frac{du}{F_2(u)+A}\right] \tag{6.5}$$

for $z < z^*$, where

$$z^* = \frac{1}{2\pi}\int_0^{\frac{1}{2}}\frac{du}{F_1(u)},$$

and $\overline{u}_1(\omega,\theta)$ (respectively, $\overline{u}_2(\omega,\theta)$) is the solution of

$$\theta = \frac{\omega}{2\pi}\int_0^{\overline{u}_1(\omega,\theta)}\frac{du}{F_1(u)},$$

respectively,

$$\theta = \frac{\omega}{2\pi}\left[\int_0^{\frac{1}{2}} \frac{du}{F_1(u)} + \int_{\frac{1}{2}}^{\bar{u}_2(\omega,\theta)} \frac{du}{F_2(u)}\right].$$

Here the subscript on $\mathcal{F}^+$ denotes the path in Fig. 9.

The solutions of the equations $\mathcal{F}^{\pm} = 0$ generically generate two distinct curves that emanate from every point $(\omega, \theta) = (m\omega_0/n, 0)$ and bound the resonance zone $\mathcal{R}_{n/m}$. The following proposition gives some information on the global (in (ω, θ)) disposition of these zones for any fixed $A \in (A_0, A_1)$.

PROPOSITION 1.

(i) *$\mathcal{R}_{n/m}$ does not intersect the line $\theta = 1$ for $\omega > 0$.*

(ii) *$\rho = \infty$ along the line $\omega = 0$ for $\theta \in (0, 1)$.*

(iii) *If $r \neq km$ and $s \neq kn$ for some $k \in \mathbf{Z}$, then*

$$\mathcal{R}_{s/r} \cap \mathcal{R}_{n/m} = \emptyset.$$

(iv) *For every fixed (m, n) $\exists\ \omega^* > 0$ $\ni$*

$$\mathcal{R}_{n/m} \subset \{(\omega, \theta) \mid \omega \leq \omega^*, \theta \in [0, 1)\}.$$

(v) *The resonance zones that emanate from the line $\theta = 0$ all terminate at $(\omega, \theta) = (0, 1)$.*

Proof. The first three facts are obvious. To prove the fourth note that when $\omega \to \infty$ the vector field tends to 0. Thus given $m > 0$ we can find $\omega^* > 0$ such that the intersections of the maximal and minimal orbits with the line $t = m$ lie below the line $u = 1/2$. To prove the fifth point we show that solutions of every rotation number exist in a sufficiently small neighborhood of the point $(\omega, \theta) = (0, 1)$.

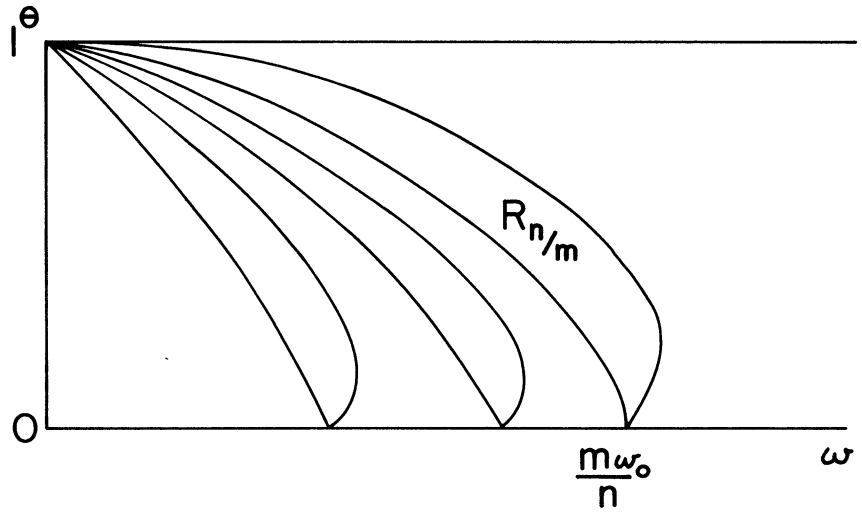

FIG. 10. *A sketch of the resonance zones in the (ω, θ) plane. ω denotes the frequency of the forcing system and θ denotes the fraction of the period during which the forcing is off. For a piecewise constant forcing the m:n resonance zone enanates from $(\omega, \theta) = (0, m\omega_0/n)$, where ω_0 is the natural frequency of the system when the forcing is on.*

Fig. 10 shows a sketch of the qualitative structure of the resonance zones for the general case. The computations involved in determining $\mathcal{F}^{\pm}$ can be carried out in detail for the piecewise-linear vector field

$$\epsilon \frac{dv}{dt} = \begin{cases} -\alpha_1 v - \beta_1 w + \gamma_1 & \text{for } v < v_l, \\ \alpha_2 v - \beta_2 w - \gamma_2 & \text{for } v \in (v_l, v_r), \\ -\alpha_3 v - \beta_3 w + \gamma_3 & \text{for } v > v_r, \end{cases} \tag{6.6}$$

$$\frac{dw}{dt} = \delta_1 v - \delta_2 w,$$

in the limit $\epsilon = 0$. The 1:1 zone is shown in Fig. 11 for a particular choice of the coefficients. We leave it to the interested reader to compute the boundaries of the resonance zone $\mathcal{R}_{n/m}$ for $(m, n) \neq (1, 1)$.

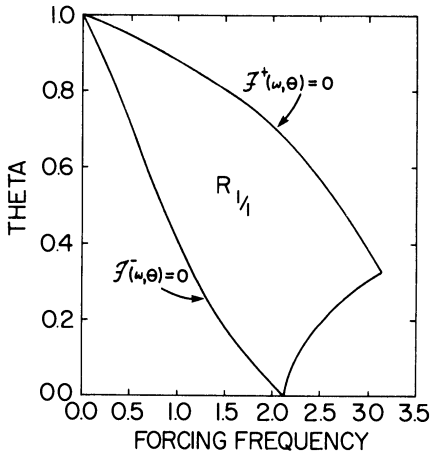

FIG. 11. *The* 1:1 *resonance zone for the piecewise linear system given by* (5.13). $\alpha_1 = 2.0$, $\alpha_2 = \alpha_3 = 1$, $\beta_i = 1$, $i = 1, c \ldots, 3$, $\gamma_1 = 0.0$, $\gamma_2 = 0.6$, $\gamma_3 = 1.8$, $\delta_1 = 1.0$, $\delta_2 = 0.5$.

Now let us consider the (θ, A) section for fixed $\omega > 0$. It is easy to show from (6.3)–(6.5) that

$$\frac{dA^-}{d\theta} = -\frac{\mathcal{F}_\theta^-}{\mathcal{F}_A^-} > 0$$

and

$$\frac{dA_i^+}{d\theta} > 0$$

for $i =$ I, II and $A - A_0$ positive and sufficiently small. Thus the forcing amplitudes corresponding to the upper and lower boundary of $\mathcal{R}_{1/1}$ are decreasing functions of the fraction of time $1 - \theta$ that the forcing is on. Earlier we showed that the time to threshold is also a decreasing function of the time the forcing is on, and these two results lead to the qualitative sketch of the amplitude-duration plane shown in Fig. 12. This diagram is in qualitative agreement with the experimental results shown in Fig. 2, except that the latter does not show the upper boundary of the 1:1 zone. A more complete analysis of the relationship between the theoretical and experimental results will be given elsewhere.

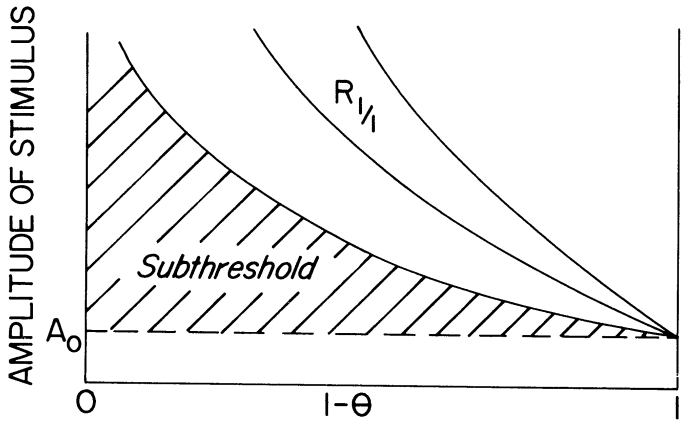

FIG. 12. *A sketch of the amplitude-duration plane for the piecewise constant forced system for A sufficiently near* A_0 (*cf. Fig.* 2(a)). *The forcing is on for a fraction* $1-\theta$ *of each period.*

7. The case $\epsilon > 0$. In the previous sections we showed that in the limit $\epsilon = 0$ the dynamical behavior of the system (2.4) can be characterized by whether or not the system is in resonance with the forcing. As a parameter λ is varied, the rotation or spiking number ρ varies continuously. For a generic system the domain of λ decomposes into a disjoint set of resonance zones $\mathcal{R}_{n/m}$, on each of which the rotation number is n/m, and the union of the resonance zones is dense. In this section, we consider the case $\epsilon > 0$; that is, v is not infinitely fast. For $\epsilon > 0$, the rotation number cannot be defined to be continuous in λ. However it is to be expected that for small ϵ the dynamics approximate that of the singular limit. We prove that for $\epsilon > 0$ and λ in a resonance zone there is a stable periodic orbit that approximates the stable periodic orbit of the singular system.

THEOREM 4. *Fix* λ *in a resonance zone of the singular system and let* $Z_0(t)$ *be a stable periodic solution of this system. There is an* $\epsilon_\lambda > 0$ *such that for* $\epsilon < \epsilon_\lambda$ *there is a unique stable periodic solution* $Z_\epsilon(t)$ *of the nonsingular system such that as* $\epsilon \to 0$, *the trajectory of* $Z_\epsilon(t)$ *uniformly approaches that of* $Z_0(t)$. *Moreover, for* λ *in a compact subset of a resonance zone* ϵ_λ *can be chosen independent of* λ, *and the estimates on the nearness of* $Z_\epsilon(t)$ *to* $Z_0(t)$ *and on the stability of* $Z_\epsilon(t)$ *are uniform in* λ.

Proof. We use the machinery of singular perturbation theory applied to the asymptotics of discontinuous limit cycles. An exposition of the relevant theory is found in the book of Mishchenko and Rosov [1980], to which we refer explicitly in this section. In the language of that book, we claim that $Z_0(t)$ is a *zeroth approximation* to $Z_\epsilon(t)$. It is necessary to turn our forced system into an autonomous system in a standard way. Suppose the rotation number of the asymptotic system is p/q and that the period of the forcing is T. Introduce an angular polar variable τ and radial

variable r, and extend the system to the following one:

$$\begin{aligned} \epsilon \frac{dv}{dt} &= f(v, w, \lambda), \\ \frac{dw}{dt} &= g(v, w, \lambda, \tau) \\ \frac{d\tau}{dt} &= 2\pi/T, \\ \frac{dr}{dt} &= r(1-r). \end{aligned} \tag{7.1}$$

Since g is periodic in its third variable, the system is well-defined on 4-dimensional space. The last two variables do not depend on the first two and the subsystem of the last two variables has a unique stable periodic orbit with $r \equiv 1$. Clearly periodic orbits of this autonomous system correspond with periodic orbits of the periodically forced system (2.4). For purposes of understanding the proof, and in particular the pictures in Mishchenko and Rosov [1980], it is convenient to suppose that $q = 1$, but the argument works for arbitrary q.

On page 173 of Mishchenko and Rosov [1980], there are five conditions which must hold for the results to hold. We discuss these five conditions in our context. The surface (3-dimensional in our case) Γ is the locus of the equation $f(v, w, \lambda) = 0$. A nonregular point is a point on Γ where $\partial f/\partial v = 0$; i.e., where the graph of f is horizontal. A nonregular point $S \in \Gamma$ with coordinates (v_0, w_0, τ_0, r_0) is called a junction point if the five conditions are satisfied. Let $G(v, w, \tau, r)$ denote the right-hand side of the last three equations in (7.1). Given (w_0, τ_0, r_0), let $X^1_{w_0,\tau_0,r_0}$ be the line consisting of the points

$$\{(v, w_0, \tau_0, r_0) : -\infty < x < \infty\}.$$

(a) S is not a zero of G (the word "not" is dropped in Mishchenko and Rosov [1980]). This is always the case since $dt/d\tau$ is never zero.

(b) All eigenvalues of the matrix $\left(\partial f/\partial v\right)$, except one, which vanishes, have negative real parts. This is vacuous in our case since the matrix has size (1×1).

(c) For v, τ, and r fixed at v_0, τ_0, and r_0, respectively, the equation

$$\epsilon \frac{dv}{dt} = f(v, w_0, \lambda) \tag{7.2}$$

has only one trajectory approaching S when $t \to -\infty$. This is clear in our case.

(d) No line in R^4 obtained by the translation of the line $X^1_{w_0,\tau_0,r_0}$ by the vector $h \cdot G(S)$ ($h > 0$ sufficiently small, but independent of ϵ) contains equilibrium positions of (7.2) near S in R^4. (This condition is mistranslated in Mishchenko and Rosov [1980]. The intent is that locally the 2-dimensional sections obtained by fixing τ and r look like Figs. 26 and 27 on page 43 of Mishchenko and Rosov [1980]. Orbits near the junction point for $\epsilon > 0$ must "fall away from" the $f = 0$ surface, and so their behavior is governed by the fast part of the trajectory of the orbit for $\epsilon = 0$.) This condition is verified so long as the w-nullcline does not intersect critical points of the v-nullcline. Note that a trajectory of (2.4)

with $\epsilon = 0$ (considered as an orbit of (7.1) with $\epsilon = 0$) contains only junction points as nonregular points precisely if it a periodic resonant orbit.

Finally there is a *drop-point condition*: the orbit of (7.2) which approaches S as $t \to -\infty$ approaches a stable (in v) point of Γ as $t \to \infty$; this condition is always satisfied in our case. Thus all conditions except (d) are satisfied in general by (7.1), and (d) is satisfied precisely if the system is resonant.

In Chapter V of Mishchenko and Rosov [1980], periodic solutions are investigated. There are additional assumptions (p. 199) that the asymptotic system has a periodic solution Z_0, which (p. 200) is isolated and stable. There is a nondegeneracy condition (p. 202) which is a linearized version of (d) above and like (d) is satisfied when the system is resonant. Accordingly, Theorem 1 on page 204 of Mishchenko and Rosov [1980] guarantees that there is a periodic solution Z_ϵ for small $\epsilon > 0$ which uniformly approaches Z_0 as $\epsilon \to 0$.

Next we investigate the stability of Z_ϵ by obtaining information about the Floquet exponents of the orbit Z_ϵ. The variational matrix of (7.1) is clearly

$$\begin{pmatrix} \frac{1}{\epsilon}\frac{\partial f}{\partial v} & \frac{1}{\epsilon}\frac{\partial f}{\partial w} & 0 & 0 \\ \frac{\partial g}{\partial v} & \frac{\partial g}{\partial w} & \frac{\partial g}{\partial \tau} & 0 \\ 0 & 0 & 0 & 0 \\ 0 & 0 & 0 & -1 \end{pmatrix}.$$

The Floquet exponents are the eigenvalues of the integral of this matrix along the orbit. There is one 0 eigenvalue and one equal to -1; we need to show that the others are in the negative half-plane. Clearly the bottom right corner splits off and we consider the (3×3) upper left corner. There is an easily verified criterion for a (3×3) matrix to have one zero eigenvalue and two in the negative half-plane. Let σ_1 denote the trace of the matrix, σ_3 the determinant, and σ_2 the sum of the three (2×2) principal minors (the characteristic polynomial is then $t^3 - \sigma_1 t^2 + \sigma_2 t - \sigma_3$). The condition is: $\sigma_1 < 0$, $\sigma_2 > 0$, and $\sigma_3 = 0$. In our case we compute

$$\sigma_1 = \oint_{Z_\epsilon} \left[\frac{1}{\epsilon}\frac{\partial f}{\partial v} + \frac{\partial g}{\partial w}\right] dt,$$

$$\sigma_2 = \frac{1}{\epsilon}\oint_{Z_\epsilon} \left[\frac{\partial f}{\partial v}\frac{\partial g}{\partial w} - \frac{\partial f}{\partial w}\frac{\partial g}{\partial v}\right] dt.$$

The computation of σ_1 proceeds as on page 142 of Mishchenko and Rosov [1980] (where the integral is computed to show stability for a two-dimensional system). The computation of σ_2 is easier, because the integrand is independent of ϵ. The integrand has to be positive by continuity, since for $\epsilon = 0$, the "value" of σ_2 is $+\infty$, because Z_0 is stable. Accordingly the three nonzero Floquet exponents lie in the negative half-plane and Z_ϵ is stable.

Finally we note that all the estimates of Mishchenko and Rosov [1980] depend on how well condition (d) (and for stability, the later linearized version) is satisfied. If λ lies in some compact subset of a resonance interval, on the periodic orbits of the asymptotic systems the w-nullcline is bounded away from the critical points of the v-nullcline. Accordingly, the estimates can be made uniform in λ, with the resulting uniformity of the theorem. This completes the proof of the theorem.

Of course around the edges of the resonant sets in the parameter space, as ϵ is increased from 0, the behavior is not described by this result. The picture becomes fuzzy, literally so if one is plotting return maps. Other types of analysis will be required to understand the behavior in these regions.

8. Numerical results for the Fitzhugh-Nagumo equations. If (2.12) admits an asymptotically stable periodic orbit then Theorem 4 implies that (2.4) does also for sufficiently small ϵ. The bound on ϵ is not uniform but depends on a number of factors, one of which is the denominator n of m/n. We expect that as the parameter λ is varied in (2.4) when ϵ is sufficiently small we may see a complicated bifurcation sequence in the region between parameter values where there is m-fold spiking and m'-fold spiking. The invariant sets will include at least periodic orbits with rotation numbers m/n with n larger (possibly considerably larger) than 1. In this section we give some numerical results that illustrate some of these transitions.

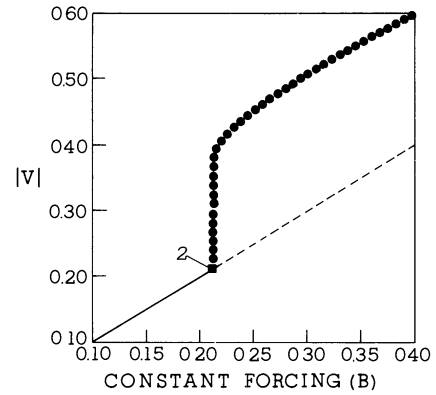

FIG. 13. *The bifurcation diagram for the Fitzhugh-Nagumo equations* (8.1) *with constant forcing. The horizontal axis is the forcing amplitude b. The vertical axis is the scaled* L_2*-norm* $|v| \equiv \{\frac{1}{T}\int_0^T v(t)^2 dt\}^{1/2}$. *The stationary point* (v, w) *is stable when b is small (the solid curve), but becomes unstable (dashed curve) through a Hopf bifurcation (the solution point with label* 2*). The bifurcating branch of periodic solutions (the branch of solid circles) is supercritical and the periodic solutions are therefore asymptotically stable. This and the succeeding two figures were generated by the numerical bifurcation package* AUTO (*Doedel* [1981]).

The equations we consider are the Fitzhugh–Nagumo equations (Fitzhugh [1969]) with sinusoidal forcing :

$$\begin{aligned} \epsilon \frac{dv}{dt} &= F(v) - w, \qquad F(v) \equiv v(v-a)(1-v) \\ \frac{dw}{dt} &= v - dw - \big(b + r\sin(\beta t)\big). \end{aligned} \tag{8.1}$$

The vector field for this system is similar to that shown in Fig. 3. Throughout this section we fix $\epsilon = 0.005$, $a = 0.5$, and $d = 1.0$.

First consider the effect of constant forcing, i.e., set $r = 0$ and treat b as the bifurcation parameter. The behavior of the solutions is summarized in Fig. 13, which shows a scaled L_2-norm $|v| \equiv \{T^{-1}\int_0^T v(t)^2 dt\}^{1/2}$ as a function of the forcing amplitude b.

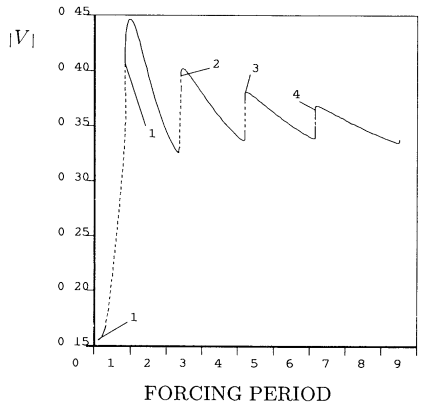

FIG. 14. *A portion of the branch of periodic solutions as a function of the period T of the forcing. The vertical axis is the norm $|v|$. The labels on the curve indicate the number of spikes (large excursions in v) per period of the forcing function. Solid lines denote stable periodic solutions and dashed lines denote unstable periodic solutions. New spikes form continuously along the primary branch but the solutions are unstable in some regions. Other solutions which exhibit higher resonance or are chaotic, are seen if the system is allowed to evolve. Further details on the solution set in the transition region between* 1 *and* 2 *spikes are given in Fig.* 15.

The stationary point (v, w) is stable when b is small (the solid curve in Fig. 13), but becomes unstable (dashed curve) through a Hopf bifurcation (the solution point with label 2). The bifurcating branch of periodic solutions is supercritical and the periodic solutions are therefore asymptotically stable.

Next we fix b at $b = 0.2$, i.e., just to the left of the Hopf bifurcation point in Fig. 13, which implies that the rest point of (8.1) is stable when $r = 0$. Now suppose that $r \neq 0$, i.e., the time-dependent component of the forcing is nonzero. For sufficiently small r there is a small amplitude stable periodic solution without spikes, but when r is sufficiently large ($>\sim 0.06$) the periodic forcing term will have values to the right of the Hopf bifurcation point during a fraction of the forcing period, and large amplitude excursions (spikes) may exist. The spiking behavior over a range of β-values for $r = 0.2$ is illustrated in Fig. 14, where $|v|$ is shown versus the forcing period $T \equiv 2\pi/\beta$. The solid portions of the single, smooth solution curve in Fig. 14 correspond to asymptotically stable periodic solutions, and the dashed portions represent unstable solutions. When the period of the forcing function is small (i.e., high forcing frequency) there is no spiking. This corresponds to the solutions of small norm at the lower left of Fig. 14. The labels in the diagram indicate the number of spikes per forcing period for nearby solution points on the branch. With respect to (2.8), note that

$$v_l = \frac{1 + a - \sqrt{a^2 - a + 1}}{3},$$

$$\gamma''(v_l) = \frac{1}{\sqrt{a^2 - a + 1}},$$

$$\left|g_t(v_l, w_l, T_1)\right| = \beta\sqrt{r^2 - (b - v_l + dw_l)^2}.$$

It can be checked that (8.1) satisfies (2.8) for the parameter values used here when $\beta > 1.14\cdots$.

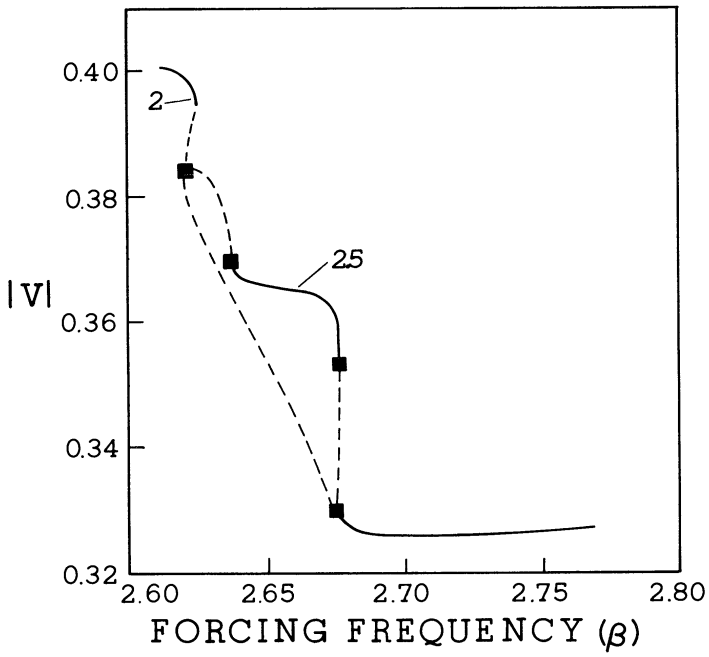

FIG. 15. *An enlargement of the transition region between one and two spikes. Solid lines denote stable periodic solutions, dashed lines denote unstable periodic solutions, and solid squares denote period-doubling bifurcations. Note that the horizontal axes in Figs.* 15 *and* 16 *are different (the former is period; the latter is frequency). The diagram shows the main branch and a secondary period-doubled branch of periodic solutions. Solutions on the main branch at the right have one spike per forcing period. At the rightmost secondary bifurcation point* ($\beta \sim 2.675$) *the solution has alternating full spikes and subthreshold responses. During the nearly-vertical portion of the secondary branch, a second spike is formed every other forcing period; this solution is stable (label* 2.5*). Further to the left there is another period doubling bifurcation followed by a gap in which neither of the solutions shown is stable. Further period-doublings also occur on branches that emanate from the secondary branch. Plots of solutions obtained by numerical integration are shown in Fig.* 17.

The solution curve in Fig. 14 contains several saddle-node bifurcations (limit points) and period doubling bifurcations. The latter have not been indicated. However, in Fig. 15 we show some of the period doubling behavior that occurs in the transition region from 1- to 2-spike solutions as a function of the forcing frequency β (note that the independent variable is changed from the previous figure in order to emphasize the region of interest). Label 2 in Fig. 15 corresponds to the same solution as label 2 in Fig. 14. The solid squares denote period doubling bifurcations, and one of the resulting additional solution branches is also shown. It contains a region of stable periodic behavior (the solid curve near label 2.5) and further period doubling bifurcations. An entire sequence of such bifurcations is possible. In fact we have traced out additional bifurcating branches, but for the sake of clarity these are not shown in the diagram.

It is clear from Figs. 14 and 15 that there exists a continuous transition along the primary branch from 1 spike to 2 spikes in which an additional spike grows smoothly. However, at a certain stage of the spike-building process this transition becomes un-

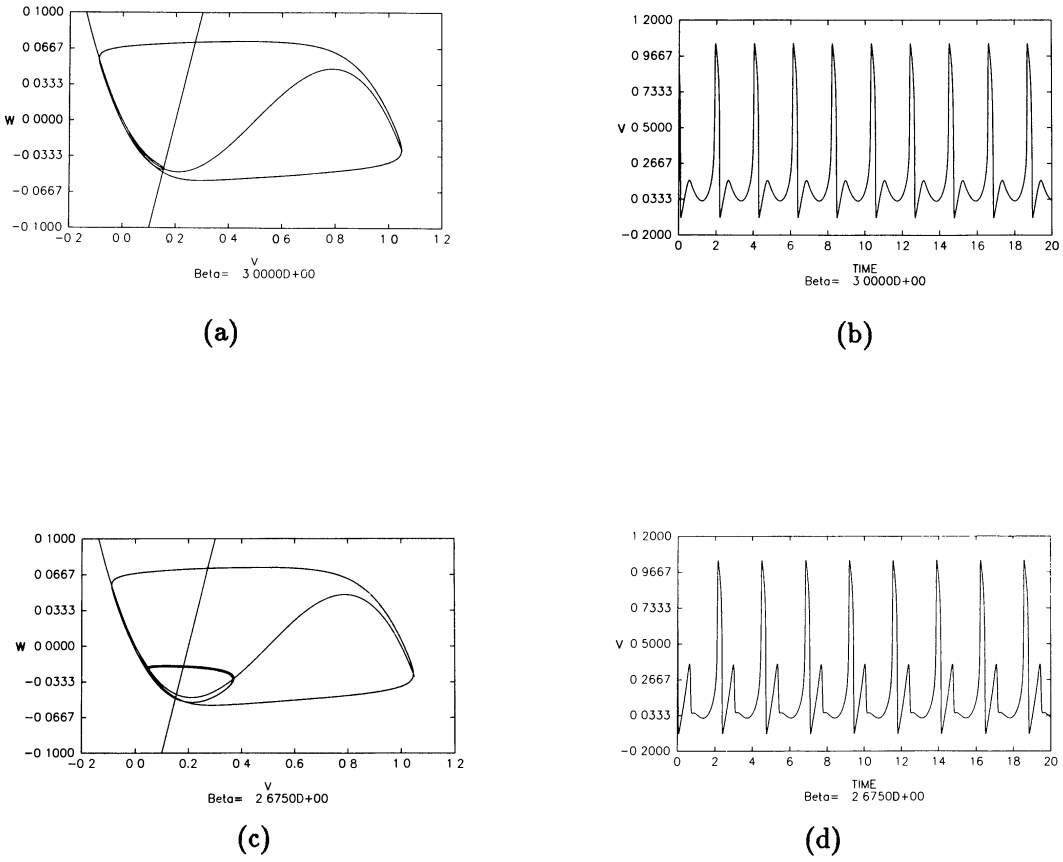

FIG. 16 (see also continuation). *The projection of the orbits into the v-w plane and the v-component of the solution as a function of time for various values of* β. (a) *and* (b): $\beta = 3.0$, (c) *and* (d): $\beta = 2.675$, (e) *and* (f): $\beta = 2.65$, (g) *and* (h): $\beta = 2.625$. *The solution at* $\beta = 3.0$ *has one spike per forcing period and is on the main branch of Fig.* 14. *In the asymptotic limit* $\epsilon = 0$ *this solution would reduce to one with rotation number* 1. *The solution at* $\beta = 2.675$ *still has one spike per forcing period but one sees in Fig.* 17(c) *that the subthreshold response is becoming erratic. The solution at* $\beta = 2.65$ *alternates between one and two full spikes per forcing period. This would correspond, in the limit* $\epsilon = 0$, *to a solution with rotation number* 3/2. *Finally, the solution at* $\beta = 2.625$ (*Fig.* 17 (g) *and* (h)) *is either chaotic or has a very high period* (*longer runs show no apparent periodicity, but we have not examined this carefully*).

stable via a period-doubling bifurcation. The foregoing results suggest that the stable behavior may consist of a cascade of period doublings that lead to chaos. In order to understand how the sensitive dependence on initial data that characterizes chaotic behavior can arise in this system, we have computed the solutions by integration of the differential equations for a sequence of β values that cover the range in which the basic solution branch is unstable. Some of the results are shown in Fig. 16. This sequence shows the stable solution and how it evolves as the frequency is decreased. At $\beta = 3.0$ (Fig. 16(a) and (b)) there is a stable solution with one complete spike and a subthreshold response. As the frequency decreases below the first period-doubling point the subthreshold response grows and the stable solution consists of alternate

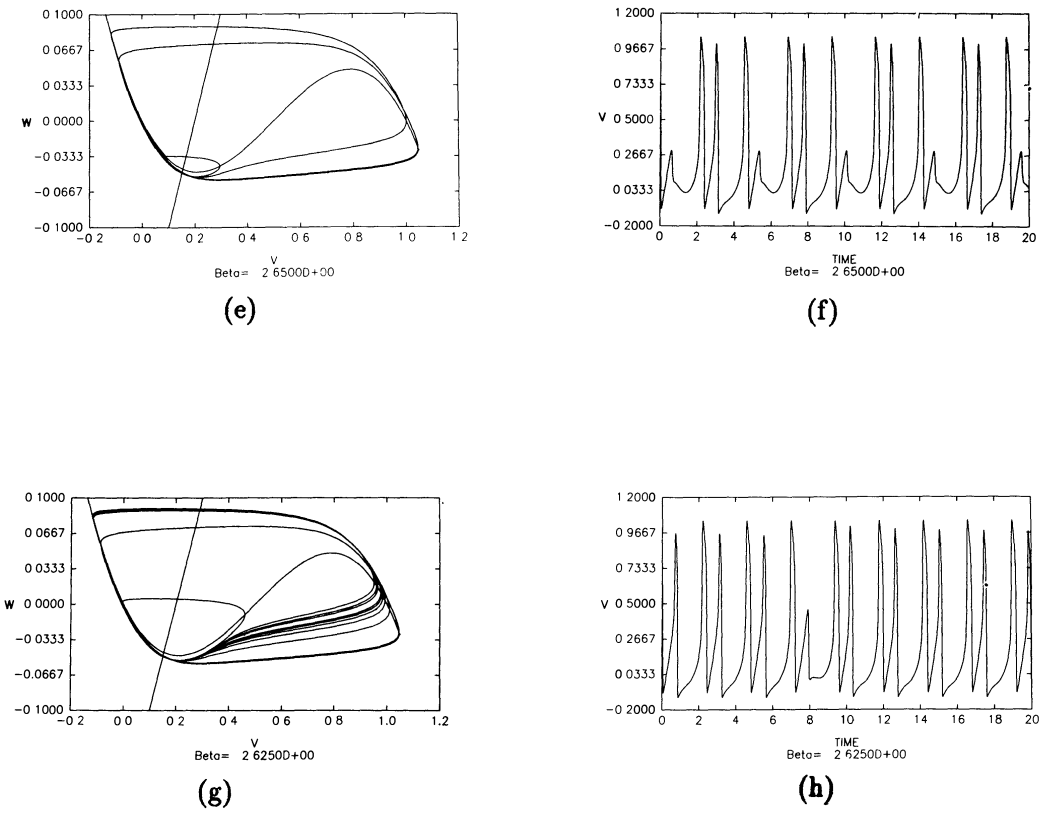

FIG. 16 (continued). *Graphs* (e)–(h).

full and partial spikes (Fig. 16(c) and (d)). When β is decreased to a value in the interval where the secondary branch is stable the stable solution consists of an alternation between one and two spikes per forcing period (Fig. 16(e) and (f)). When β lies in the interval where the primary and secondary branches are both unstable the solution is either chaotic or has a very long period (Fig. 16(g) and (h)). As the frequency decreases further another partial spike begins to grow, entering a region in which the basic solution of two full spikes and a partial spike becomes unstable, and the foregoing sequence continues until there are three complete spikes.

The projections into the v-w plane show where the sensitivity of the orbits arises and how this may lead to chaos. As a partial spike grows, the trajectory approaches a separatrix between a full and a partial spike, corresponding to the trajectory through the rightmost turning point in the v nullcline. Trajectories that cross the separatrix produce large spikes, while those that fall below produce partial spikes, and since the system is quite stiff for the chosen value of ϵ, the transition between these possibilities depends sensitively on the forcing when the orbit is near the separatrix. Clearly this does not preclude building a spike continuously, as happens along the continuous curve in Fig. 15, but it cannot be done in a dynamically stable manner because of the sensitivity. It is difficult to do more analytically for the Fitzhugh–Nagumo equations,

but more can be done for a piecewise-linear vector field and piecewise-constant forcing. Analytical and numerical results for this problem will be reported elsewhere.

9. Discussion. In the singularly-perturbed limit the two-dimensional system of equations that models an excitable system reduces to a discontinuous vector field on the circle. Under periodic forcing such a system leads to a discontinuous vector field on a torus, and as we have shown, we can develop a theory for such systems that closely parallels the classical theory for smooth flows. Our approach is novel in that the theory is not restricted to small amplitude forcing. This generality is gained at the expense of reducing the full system to its singular limit, which precludes the possibility of anything more complicated than quasi-periodic behavior. However our analysis is sufficiently general to include as a special case the type of integrate-and-fire models developed in Rescigno et al. [1970], Builder and Roberts [1939], and Glass and Mackey [1979], and further analyzed in Keener, Hoppensteadt, and Rinzel [1981]. In fact, a figure essentially identical to our Fig. 10 is given in Builder and Roberts [1939], although previous work was aimed at understanding forced periodic systems and thus did not deal with the existence of threshold phenomena. The introduction of the critical shadow for the flow enables us to connect our results more closely with the classical theory, for, as we showed, there is a saddle-node bifurcation on the boundary of the phase-locking region in our theory. In contrast, if we do not treat the circle map as set-valued (or alternatively, do not consider the critical shadow for the flow), we lose a root at the discontinuity of the associated circle map and there is no obvious connection with the bifurcation structure of the smooth case (Glass and Mackey [1979]; Keener [1980]; Keener, Hoppensteadt, and Rinzel [1981]). Furthermore, our approach is necessary in order to connect the dynamics in the singularly-perturbed ($\epsilon = 0$) limit with the dynamics in the $\epsilon > 0$ case. The numerical results on the Fitzhugh–Nagumo equations given in §8 illustrate how spikes in a stiff but not singularly-perturbed system are built, and in particular, they show how the existence of a threshold can lead to an instability in the spike-building process. In this paper we analyzed the time-one map of the flow, but we could also have analyzed the mapping from $u = 0$ to $u = 1$ defined by the flow (cf. Fig. 7(a)). It is easy to see that this phase map is discontinuous and multiple-valued for $\epsilon = 0$, and extends to a discontinuous self-mapping of a cylinder for $\epsilon > 0$. We shall show elsewhere that we can analyze much of the structure in the transition region between the n- and $(n + 1)$-spike regions when $\epsilon > 0$ for a piecewise linear vector field using this cylinder map.

Another observed phenomenon which has been analyzed in terms of excitable systems is bursting. If a dynamical system is excitable for some values of the parameters that system will often have self-sustained periodic solutions for nearby parameter values. Thus if a parameter is varied slowly to switch such a system periodically between a regime in which it is excitable and a regime in which it is oscillatory, another type of dynamical behavior called *bursting* is observed. Bursting is a form of periodic or aperiodic behavior characterized by a number of large excursions that are closely spaced in time, separated by intervals of quiescence. Roughly speaking, one period in a periodic bursting system comprises one or more rapid excursions through the amplifying set and slow variation in the decaying set.

Usually bursting is modelled with an autonomous system, which more-or-less naturally separates into a "slow" forcing subsystem and a "fast" response subsystem, possibly with a small amount of feedback from the response subsystem to the forcing subsystem. Bursting is known to occur in molluscan neurons (Adams and Benson [1985];

Alving [1968]), in hippocampal cells (Johnson and Brown [1984]), in pancreatic β-cells (Atwater et al. [1980]; Chay and Keizer [1983]), and in the Zhabotinskii–Belousov reaction (Hudson, Hart, and Marinko [1979]; Janz, Vanacek, and Field [1980]). An example of the output recorded in a bursting system is shown in Fig. 17. When viewed as the result of slow forcing of an excitable system, periodic solutions of this type are superharmonics in the usual terminology in that the system "fires" more than once per cycle of the forcing function. Many models of bursting systems involve a differential system which is far from a singular limit, and there are thus differences in the detailed structure of the spiking. However, the coarse behavior is well-modelled by a system at or near the singular limit, and better agreements can be expected with further results in the case $\epsilon > 0$, especially if ϵ is far from zero. As we note below, the effect of feedback does not alter the qualitative behavior of a forced excitable system, except near the boundaries of the resonance zones.

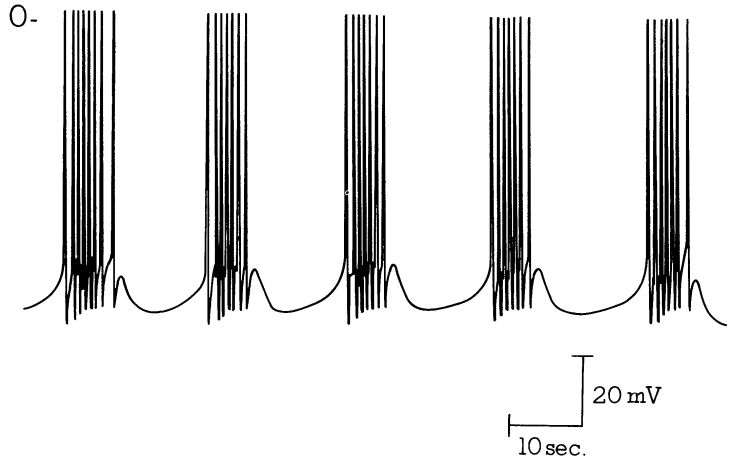

FIG. 17. *The transmembrane potential as a function of time recorded in the bursting* R15 *neuron of Aplysia californica.*

One of the earliest models for bursting in neurons is that of Plant and Kim (Plant [1978]; Plant [1981]; Plant and Kim [1976]). Since then there have been many models proposed for other bursting systems (Chay [1986]; Chay and Rinzel [1985]; Rinzel [1985]) and numerous analyses of bursting (Argemi et al. [1984]; Argemi, Gola, and Chagneux [1979]; Argemi, Gola, and Chagneux [1980]; Baer and Tier [1986]; Decroly and Goldbeter [1987]; Ermentrout and Kopell [1986]; Honerkamp, Mutschler, and Seitz [1985]; Rinzel [1987]; Rinzel and Lee [1986]; Rinzel and Lee [1987]). These have relied either on perturbation analysis valid for small perturbations of a fixed system (Ermentrout and Kopell [1986]) or on a multiple-time-scale analysis (Argemi et al. [1984]; Argemi, Gola, and Chagneux [1979]; Argemi, Gola, and Chagneux [1980]; Honerkamp, Mutschler, and Seitz [1985]; Rinzel and Lee [1987]). In most cases the foregoing authors treat dynamical systems comprised of slow and fast subsystems with bilateral coupling between them. As was just suggested, an alternate viewpoint is to regard the bursts as superharmonic solutions in a slowly-forced excitable system in which the spike-generating system has no influence on the slow forcing system. One of our long-term objectives is to determine whether such a model is adequate to explain the experimental observations on bursting, or whether there are observed phenomena that can only be understood in the framework of a coupled system. Our immediate

objective in studying these types of solutions is to understand how the number of "spikes," or large excursions in a burst, changes as parameters in the equations are varied. Our approach is close to that of Ermentrout and Kopell [1986], but our results are not restricted to small perturbations of degenerate systems. Moreover, the results will be applicable to forced excitable systems in general.

Our analysis of a forced system is based on slow forcing of an excitable system, and does not require any feedback from the fast to the slow system, as is present in many bursting systems. The motivation for doing this is two-fold. Firstly, it is easier from the mathematical standpoint to analyze forced excitable systems. Secondly, we can imagine many slow external periodic influences, such as the light-dark cycle or internal rhythms uncoupled from the bursting system, which could provide the forcing but which are in no way influenced by the responding system. This observation may be important in the brain, for it shows how a supersensitivity to a global signal can lead to large-scale synchronized activity. There are of course examples in which there is feedback from the slow to the fast system, and it is possible to analyze such a coupled system in terms of general results about (bi-)coupled oscillators. In analyses which consider one system as forced by the other, the feedback is weak is and is effectively eliminated in the mathematics by normal forms or some other technique. The following general considerations show that weak feedback does not introduce new qualitative features in the interior of phase-locking regions. In a system with feedback the forcing itself is weakly state-dependent, which can be modelled as follows. We consider an autonomous system

$$\begin{aligned} \epsilon \frac{dv}{dt} &= f(v, w, z), \\ \frac{dw}{dt} &= g(v, w, z), \\ \frac{dz}{dt} &= h\big(k_\eta(v, w), z\big), \end{aligned} \tag{9.1}$$

where z may have more than one component. We regard this as the forcing subsystem, and $k_\eta(v, w)$ represents the feedback. Let the magnitude of the feedback be measured by η and suppose that $k_0(v, w) = 0$, in which case there is no feedback. We assume that for $\eta = 0$, the system

$$\frac{dz}{dt} = h(0, z)$$

has a stable periodic orbit $\phi(t)$. In this case (9.1) reduces to (2.1), and the theory we have developed applies. If the reduced system with $\epsilon = 0$ is resonant for $\eta = 0$, then for small $\epsilon > 0$, the system has a stable periodic orbit. Thus by regular perturbation theory, for small η (depending on ϵ), the system (9.1) has a stable periodic orbit. In other words, feedback does not alter the qualitative dynamics when the parameters lie in the interior of a a resonance zone. Feedback is likely to have a more profound effect near the boundaries of the resonant parameter sets, and in it may be that it provides one mechanism for effecting chaotic behavior.

Appendix.

Normal form for forcing. In §2, we considered systems in the normal form

$$\begin{aligned} \epsilon \frac{dv}{dt} &= f(v, w, \lambda), \\ \frac{dw}{dt} &= g(v, w, \lambda, t). \end{aligned}$$

That is, the forcing is on the second, slow variables. In this appendix, we show that a number of systems with the forcing on the first variable can be normalized to this form. Thus consider

$$\begin{aligned} \epsilon\frac{dv}{dt} &= f\big(v,w,\phi(t)\big) = p(v) - q\big(w,\phi(t)\big), \\ \frac{dw}{dt} &= g(v,w,\psi(t)), \end{aligned} \tag{A.1}$$

where

$$\begin{aligned} p &: R^m \to R^m, \\ q &: R^n \times R^1 \to R^m, \\ g &: R^m \times R^n \times R^1 \to R^n. \end{aligned} \tag{A.2}$$

We assume for the present that p, q, and g are C^1, by which is meant that p, q, and g have continuous bounded derivatives on their respective domains. In order to transfer the forcing from the v equations to the w equations we want to define the new variable $\tilde{w} \equiv q\big(w,\phi(t)\big)$ and then invert this relation to obtain w in terms of $\tilde{w}$ and ϕ. To do this we have to regard q as an abstract map and use a global implicit function theorem on suitable spaces.

Let $R^+ \equiv [0,\infty)$ and let $C(R^+,R^k)$ be the set of continuous bounded functions on R^+ with values in R^k, endowed with the norm $\|u\|_\infty = \sup_{[0,\infty)} \|u(t)\|_k$. Let $C^1(R^+,R^k)$ be the set of functions in $C(R^+,R^k)$ with continuous bounded derivatives, and let C_T be the set of continuous real-valued T-periodic functions endowed with the norm $\|\phi\|_\infty = \max_{[0,T]} |\phi(t)|$. Then the function q in (A.2) gives rise to the substitution operator

$$\mathcal{Q} : C(R^+,R^n) \times C_T \to C(R^+,R^m).$$

defined by

$$\mathcal{Q}(w,\phi)(t) = q(w(t),\phi(t)).$$

This operator inherits the regularity of the associated function on $R^n \times R^1$, as is shown in the following proposition.

PROPOSITION 1. *Let $f \in C^1(R^1,R^1)$ and let $\mathcal{F} : C(R^+,R^1) \to C(R^+,R^1)$ be the substitution operator defined by*

$$\mathcal{F}(u)(t) \equiv f\big(u(t)\big)$$

for $u \in C(R^+,R^1)$. Then $\mathcal{F} \in C^1\big(C(R^+,R^1),C(R^+,R^1)\big)$.

Proof. Since $f \in C^1(R^1,R^1)$,

$$f(x+y) - f(x) = \int_0^1 f'(x+sy)y\,ds$$

and therefore

$$\mathcal{F}(u_0+\xi)(t) - \mathcal{F}(u_0)(t) = \int_0^1 f'(u_0(t)+s\xi(t))\xi(t)\,ds$$

for any u_0 and ξ in $C(R^+, R^1)$. We claim that the Frechet derivative of $\mathcal{F}$ at u_0 is the linear operator $\mathcal{F}'$ given by

$$\mathcal{F}'(u_0)\xi = f'(u_0)\xi. \tag{A.3}$$

Clearly

$$\mathcal{F}(u_0+\xi) - \mathcal{F}(u_0) - f'(u_0)\xi = \xi\Big(\int_0^1 f'(u_0+s\xi)\,ds - \int_0^1 f'(u_0)\,ds\Big)$$

and thus

$$\|\mathcal{F}(u_0+\xi) - \mathcal{F}(u_0) - f'(u_0)\xi\|_\infty = \|\xi\|_\infty \cdot \Big\| \int_0^1 \big(f'(u_0+s\xi)\,ds - f'(u_0)\big)\,ds\Big\|_\infty.$$

The integrand is the composition of f' with an affine map and therefore the usual rules for taking limits apply. It follows that the right-hand side is uniformly $o(\|\xi\|_\infty)$ as $\|\xi\|_\infty \to 0$. Furthermore,

$$\|\mathcal{F}'(u_0)\xi\|_\infty = \|f'(u_0)\xi\|_\infty \le \|f'(u_0)\|_\infty \cdot \|\xi\|_\infty,$$

and therefore $\mathcal{F}'$ as defined by (A.3) is bounded. Consequently it is the Frechet derivative of $\mathcal{F}$ at u_0. It is clear that if $f'(x)$ is nonvanishing for all $x \in R$ then $\mathcal{F}'$ is an isomorphism at u_0.

The foregoing implies that the Frechet derivative of $\mathcal{Q}$ at (w_0, ϕ_0) is given by

$$\mathcal{Q}'(w_0,\phi_0)(\xi,\eta) = \frac{\partial q}{\partial w}(w_0,\phi_0)\xi + \frac{\partial q_1}{\partial \phi}(w_0,\phi_0)\eta,$$

but it is singular in general. Thus we have to consider two different cases.

First suppose that $m \ge n$. In this case we define $\tilde{w} = q(w,\phi)$ and we write $\tilde{w} = (\tilde{w}_1, \tilde{w}_2) = (q_1(w,\phi), q_2(w,\phi))$, where $\tilde{w}_1 \in R^n$, $\tilde{w}_2 \in R^{m-n}$, and q is partitioned conformally. We assume that $\partial q_1/\partial w$ is nonsingular and that $\| (\partial q_1/\partial w)^{-1} \|_n < K$ for some constant $K > 0$ and all $(w,\phi) \in R^n \times R^1$; also that $\|\partial q_1/\partial \phi\|_n$ is uniformly bounded. By the usual implicit function theorem, near any triple $(\tilde{w}_1, w, \phi)$ with $\tilde{w}_1 = q_1(w,\phi)$, there is a locally defined C^1 function $w = h(\tilde{w}_1, \phi)$ with the same graph. However, these local functions may not fit together to form a global function; that is, there may be monodromy. To preclude this, we use the following global inverse function theorem for Banach spaces (Avez [1986, Appendix D.2]).

LEMMA 1 (Hadamard–Levy). *Let E and F be Banach spaces, and let $\mathcal{F} : E \to F$ be a C^1 map. Suppose that $\mathcal{F}'(x)$ is an isomorphism for all $x \in E$, and that there is a constant $A > 0$ such that $\|[\mathcal{F}'(x)]^{-1}\| < A$. Then $\mathcal{F}$ is a diffeomorphism of E on F.*

To apply this result, let $E = F = C(R^+, R^k) \times C_T$, with norm the maximum of the component norms, and let $\mathcal{F}(w,\phi) = \big(q_1(w,\phi), \phi\big)$. Proposition 1 implies that $\mathcal{F}$ is a C^1 map with Frechet derivative

$$\mathcal{F}'(x_0)(\xi,\eta) = \left(\frac{\partial q_1}{\partial w}(w_0,\phi_0)\xi + \frac{\partial q_1}{\partial \phi}(w_0,\phi_0)\eta, \eta\right) \equiv (\zeta,\mu),$$

for any $(\xi, \eta) \in E$. Thus

$$[\mathcal{F}'(x_0)]^{-1}(\zeta, \mu) = \left(\left(\frac{\partial q_1}{\partial w}\right)^{-1}\left(\zeta - \frac{\partial q_1}{\partial \phi}\mu\right), \mu\right)$$

and it follows from the hypotheses on $\partial q_1/\partial w$ and $\partial q_1/\partial w$ that the required bound on $\|[\mathcal{F}']^{-1}\|_\infty$ exists. Thus, by the Hadamard–Levy result, there is a global inverse and so there is a unique functional $w = \mathcal{H}(\tilde{w}, \phi)$. However, locally $\mathcal{H}$ has the representation $w(t) = h\big(\tilde{w}(t), \phi(t)\big)$, and so by uniqueness, h is a global function.

Returning to the original system, for C^1 functions w and ϕ,

$$\frac{d\tilde{w}_1}{dt} = \frac{\partial q_1}{\partial w}\frac{dw}{dt} + \frac{\partial q_1}{\partial \phi}\phi',$$

and consequently (A.2) is transformed into the system

$$\begin{aligned}
\epsilon\frac{dv}{dt} &= p(v) - \tilde{w},\\
\frac{d\tilde{w}_1}{dt} &= \frac{\partial q_1}{\partial w}g\big(v, h(\tilde{w}_1, \phi(t)), \psi(t)\big) + \frac{\partial q_1}{\partial \phi}\phi'(t),
\end{aligned}$$

where $\tilde{w} = \big(q_1\big(h(\tilde{w}_1, \phi(t)), \phi(t)\big), q_2\big(h(\tilde{w}_1, \phi(t)), \phi(t)\big)\big)$. In this form the forcing only appears in the equations for the slow variables.

When $m < n$ we define $\tilde{w} = q(w, \phi(t))$ as before, and we write $w = (w_1, w_2)$. We suppose that $\partial q/\partial w_1$ is nonsingular and that the inverse of this Jacobian is uniformly bounded above. Then $w_1 = h\big(\tilde{w}, \phi(t)\big)$ and

$$\frac{d\tilde{w}}{dt} = \frac{\partial q}{\partial w}\frac{dw}{dt} + \frac{\partial q}{\partial \phi}\phi'(t).$$

Let $G\big(v, w_1, w_2, \phi(t)\big) \equiv g\big(v, (w_1, w_2), \phi(t)\big)$ and partition G to conform with the partitioning of w; then (A.2) is transformed into the system

$$\begin{aligned}
\epsilon\frac{dv}{dt} &= p(v) - \tilde{w},\\
\frac{d\tilde{w}}{dt} &= \frac{\partial q}{\partial w}G\big(v, h(\tilde{w}, \phi(t)), w_2, \psi(t)\big) + \frac{\partial q}{\partial \phi}\phi'(t)\\
\frac{dw_2}{dt} &= G_2\big(v, h(\tilde{w}, \phi(t)), w_2, \psi(t)\big).
\end{aligned}$$

The reader can verify that the foregoing simplifies when the forcing has the additive form $q(w, \phi) = q_0(w) + \phi$ with appropriate global assumptions on q_0.

Acknowledgment. The authors would like to thank John Rinzel for his valuable suggestions based on a careful reading of an earlier version of this paper.

REFERENCES

W. B. ADAMS AND J. A. BENSON, *The generation and modulation of endogenous rhythmicity in the Aplysia bursting pacemaker neuron* R15, in Progress in Biophysics and Molecular Biology, 46, D. Noble and T. L. Bundle, eds., Pergamon, Elmsford, NY, 1985, pp. 1–49.

B. O. ALVING, *Spontaneous activity in isolated somata of* Aplysia *pacemaker neurons*, J. Gen. Physiol., 51 (1968), pp. 29–45.

J. ARGEMI, H. CHAGNEUX, C. DUCREUX, AND M. GOLA, *Qualitative study of a dynamical system for metrazol-induced paroxysmal depolarization shifts*, Bull. Math. Biol., 46 (1984), pp. 903–922.

J. ARGEMI, M. GOLA, AND H. CHAGNEUX, *Qualitative analysis of a model generating long potential waves in Ba-treated nerve cells*—I. *Reduced systems*, Bull. Math. Biol., 41 (1979), pp. 665–686.

———, *Qualitative analysis of a model generating long potential waves in Ba-treated nerve cells*—II. *Complete systems*, Bull. Math. Biol., 42 (1980), pp. 221–238.

I. ATWATER, C. M. DAWSON, A. SCOTT, G. EDDLESTONE, AND E. ROJAS, *The nature of the oscillatory behavior in electrical activity for the pancreatic β-cell*, J. of Hormone and Metabolic Res., Suppl., 10 (1980), pp. 100–107.

A. AVEZ, *Differential Calculus*, John Wiley, New York, NY, 1986.

S. M. BAER AND C. TIER, *An analysis of a dendritic neuron model with an active membrane site*, J. Math. Biol., 23 (1986), pp. 137–161.

G. BUILDER AND N. F. ROBERTS, *The synchronization of a simple relaxation oscillator*, AWA Tech. Rev., 4 (1939), pp. 164–180.

T. R. CHAY, *Oscillations and chaos in the pancreatic β-cell*, in Nonlinear Oscillations in Biology and Chemistry, H. G. Othmer, ed., Lect. Notes in Biomath. 66, Springer-Verlag, New York, Heidelberg, Berlin, 1986, pp. 2–18.

T. R. CHAY AND J. KEIZER, *Minimal model for membrane oscillations in the pancreatic β-cell*, Biophys. J., 42 (1983), pp. 181–190.

T. R. CHAY AND J. RINZEL, *Bursting, beating, and chaos in an excitable membrane model*, Biophys. J., 47 (1985), pp. 357–366.

D. R. CHIALVO AND J. JALIFE, *Non-linear dynamics of cardiac excitation and impulse propogation*, Nature, 330 (1987), pp. 749–752.

E. A. CODDINGTON AND N. LEVINSON, *Theory of Ordinary Differential Equations*, McGraw-Hill, New York, NY, 1955.

O. DECROLY AND A. GOLDBETER, *From simple to complex oscillatory behavior: Analysis of bursting in a multiply regulated biochemical system*, J. Theoret. Biol., 124 (1987), pp. 219–250.

A. DENJOY, *Sur les courbes définies par les équations différentielles à la surface du tore*, J. de Math., 11 (1932), pp. 333–375.

E. J. DOEDEL, AUTO: *A program for the automatic bifurcation and analysis of autonomous systems*, Congr. Numer., 30 (1981), pp. 265–284.

G. B. ERMENTROUT AND N. KOPELL, *Parabolic bursting in an excitable system coupled with a slow oscillation*, SIAM J. Appl. Math., 46 (1986), pp. 233–253.

M. FEINGOLD, D. L. GONZALEZ, O. PIRO, AND H. VITURRO, *Phase locking, period doubling and chaotic phenomena in externally driven excitable systems*, Phys. Rev. A (3), 37 (1988), pp. 4060–4063.

R. J. FIELD AND R. M. NOYES, *Oscillations in chemical systems*, IV. *Limit cycle behavior in a model of a real chemical reaction*, J. Chem. Phys., 60 (1974), pp. 1877–1884.

R. FITZHUGH, *Mathematical models of excitation and propagation in nerve*, in Biological Engineering, H. P. Schwan, ed., McGraw-Hill, New York, NY, 1969, pp. 1–85.

L. GLASS AND M. C. MACKEY, *A simple model for phase locking of biological oscillators*, J. Math. Biol., 7 (1979), pp. 339–352.

J. GUCKENHEIMER AND P. HOLMES, *Nonlinear Oscillations, Dynamical Systems, and Bifurcation of Vector Fields*, Applied Mathematical Sciences 42, Springer-Verlag, New York, Heidelberg, Berlin, 1983.

R. GUTTMAN, L. FELDMAN, AND E. JAKOBSSON, *Frequency entrainment of squid axon membrane*, J. Membrane Biol., 56 (1980), pp. 9–18.

J. K. HALE, *Ordinary Differential Equations*, Pure and Applied Mathematics XXI, John Wiley, New York, NY, 1969.

G. HALL, *Resonance zones in two-parameter families of circle homeomorphisms*, SIAM J. Math. Anal., 15 (1984), pp. 1075–1081.

P. HARTMAN, *Ordinary Differential Equations*, John Wiley, New York, NY, 1964.

A. L. HODGKIN AND A. F. HUXLEY, *A quantitative description of membrane current and application to conduction and excitation in nerve*, J. Physiol., 117 (1954), pp. 500–544.

A. V. HOLDEN, *The response of excitable membrane models to a cyclic input*, Biol. Cybernetics, 21 (1976), pp. 1–7.

J. HONERKAMP, C. MUTSCHLER, AND R. SEITZ, *Coupling of a slow and a fast oscillator can generate bursting*, Bull. Math. Biol., 47 (1985), pp. 1–21.

J. L. HUDSON, M. HART, AND D. MARINKO, *An experimental study of multiple peak periodic and non-periodic oscillations in the Belousov-Zhabotinskii reaction*, J. Chem. Phys., 71 (1979), pp. 1601–1606.

J. L. HUDSON, P. LAMBA, AND J. C. MANKIN, *Experiments on low-amplitude forcing of a chemical oscillator*, J. Phys. Chem., 90 (1986), pp. 3430–3434.

R. D. JANZ, D. J. VANACEK, AND R. J. FIELD, *Composite double oscillation in a modified version of the oregonator model of the Belousov–Zhabotinsky reaction*, J. Chem. Phys., 73 (1980), pp. 3132–3138.

D. JOHNSON AND T. H. BROWN, *Mechanisms of neuronal burst generation*, in Electrophysiology of Epilepsy, P. A. Schwartzkroin and H. V. Wheal, eds., Academic Press, New York, NY, 1984, pp. 277–301.

J. P. KEENER, *Chaotic behavior in piecewise continuous difference equations*, Trans. Amer. Math. Soc., 261 (1980), pp. 589–604.

J. P. KEENER, F. C. HOPPENSTEADT, AND J. RINZEL, *Integrate-and-fire models of nerve membrane response to oscillatory input*, SIAM J. Appl. Math., 41 (1981), pp. 503–517.

W. S. LOUD, *Phase shift and locking-in regions*, Quart. Appl. Math., 25 (1967), pp. 222–227.

R. S. MACKAY AND C. TRESSER, *Transition to topological chaos for circle maps*, Phys. D, 19 (1986), pp. 206–237.

G. MATSUMOTO, K. AIHARA, Y. HANYU, N. TAKAHASHI, S. YOSHIZAWA, AND J-I. NAGUMO, *Chaos and phase locking in normal squid axons*, Phys. Lett. A, 123 (1987), pp. 162–166.

R. W. MEECH, *Membrane potential oscillations in molluscan "burster" neurons*, J. Exp. Biol., 81 (1979), pp. 93–112.

D. C. MICHAELS, E. P. MATYAS, AND J. JALIFE, *A mathematical model of the effects of acetylcholine pulses on sinoatrial pacemaker activity*, Circ. Res., 55 (1984), pp. 89–101.

N. MINORSKY, *Nonlinear Oscillations*, Van Nostrand, New York, NY, 1962.

E. F. MISHCHENKO AND N. K. ROSOV, *Differential Equations with Small Parameters and Relaxation Oscillations*, Mathematical Concepts and Methods in Science and Engineering 13, Plenum Press, New York, NY, 1980.

P. B. MONK AND H. G. OTHMER, *Cyclic* AMP *oscillations in suspensions of Dictyostelium discoideum*, Philos. Trans. Roy. Soc. London Ser. B, 323 (1989), pp. 185–224.

J-I. NAGUMO AND S. SATO, *On a response characteristic of a mathematical neuron model*, Kybernetika (Prague), 10 (1972), pp. 155–164.

S. NEWHOUSE, J. PALIS, AND F. TAKENS, *Bifurcations and stability of families of diffeomorphisms*, Inst. Hautes Études Sci. Publ. Math., 57 (1983), pp. 6–71.

H. G. OTHMER AND P. B. MONK, *Concentration waves in aggregation fields of a cellular slime mold*, in Biomathematics and Related Computational Problems, L. Ricciardi, ed., D. Reidel,

Dordrecht, Boston, London, 1988.

R. E. PLANT, *The effects of calcium on bursting neurons*, J. Neurophys., 21 (1978), pp. 217–237.

———, *Bifurcation and resonance in a model for bursting nerve cells*, J. Math. Biol., 11 (1981), pp. 11–32.

R. E. PLANT AND M. KIM, *Mathematical description of a bursting pacemaker neuron by a modification of the Hodgkin-Huxley equations*, Biophys. J., 16 (1976), pp. 227–244.

F. RATTAY, *High frequency electrostimulation of excitable cells*, J. Theoret. Biol., 123 (1986), pp. 45–54.

A. RESCIGNO, R. B. STEIN, R. L. PURPLE, AND R. E. POPPELE, *A neuronal model for the discharge patterns produced by cyclic inputs*, Bull. Math. Biophysics, 32 (1970), pp. 337–353.

J. RINZEL, *Bursting oscillations in an excitable membrane model*, in Ordinary and Partial Differential Equations, Proceedings of the eighth conference held at Dundee, Scotland, June 25–29, 1984, B. D. Sleeman and R. J. Jarvis, eds., Lect. Notes in Math. 1151, Springer-Verlag, New York, Heidelberg, Berlin, 1985, pp. 304–316.

———, *A formal classification of bursting mechanisms in excitable systems*, in Proceedings of the International Congress of Mathematics, 1986, American Mathematical Society, Providence, RI, 1987, pp. 1578–1593.

J. RINZEL AND Y. S. LEE, *On different mechanisms for membrane potential bursting*, in Nonlinear Oscillations in Biology and Chemistry, H. G. Othmer, ed., Lect. Notes in Biomath. 66, Springer-Verlag, New York, Heidelberg, Berlin, 1986, pp. 19–33.

———, *Dissection of a model for neuronal parabolic bursting*, J. Math. Biol., 25 (1987), pp. 653–675.

S. SATO, *Mathematical properties of responses of a neuron model*, Kybernetika (Prague), 11 (1972), pp. 208–216.

S. SATO, M. HATTA, AND J-I. NAGUMO, *Response characteristics of a neuron model to a periodic input*, Kybernetika (Prague), 16 (1974), pp. 1–8.